Historic England

Scientific Dating

Stour Basin, Kent
Optically Stimulated Luminescence Dating of Brickearth and Terrace Deposits

Jean-Luc Schwenninger, Martin Bates, Paul Cuming,
Elisabeth Dyson, and Francis Wenban-Smith

Discovery, Innovation and Science in the Historic Environment

Research Report Series no. 19-2015

Research Department Report Series 19-2015

STOUR BASIN
KENT

OPTICALLY STIMULATED LUMINESCENCE DATING OF BRICKEARTH AND TERRACE DEPOSITS

Jean-Luc Schwenninger, Martin Bates, Paul Cuming,
Elisabeth Dyson, and Francis Wenban-Smith

NGR: n/a

© Historic England

ISSN 2059-4453 (Online)

The Research Report Series incorporates reports by the expert teams within the Investigation & Analysis Division of the Research Department of Historic England, alongside contributions from other parts of the organisation. It replaces the former Centre for Archaeology Reports Series, the Archaeological Investigation Report Series, the Architectural Investigation Report Series, and the Research Department Report Series.

Many of the Research Reports are of an interim nature and serve to make available the results of specialist investigations in advance of full publication. They are not usually subject to external refereeing, and their conclusions may sometimes have to be modified in the light of information not available at the time of the investigation. Where no final project report is available, readers must consult the author before citing these reports in any publication. Opinions expressed in Research Reports are those of the author(s) and are not necessarily those of Historic England.

For more information write to Res.reports@HistoricEngland.org.uk
or mail: Historic England, Fort Cumberland, Fort Cumberland Road, Eastney, Portsmouth PO4 9LD

SUMMARY
A series of 20 samples were collected for optically stimulated luminescence (OSL) dating from six sites representing a range of topographic and geomorphological locations along a transect up the east side of the Blean plateau to try and provide a more secure dating framework for the brickearth and terrace deposits of the Stour Basin area in northeast Kent. Over the last century the region has produced abundant Palaeolithic remains and represents an area of high development threat. Compared to other areas of Kent such as the Lower Thames and the Medway Valley or the Thames Gateway, which have been the focus of previous Aggregates Levy Sustainability Fund projects, the Stour Basin has remained poorly studied. Given the rich and extensive Palaeolithic resources within Kent, the potentially unappreciated archaeological significance of either the Stour terrace deposits or the brickearth deposits near Thanet, Dover and Canterbury, as well as the high development pressure in these planning districts, a research project was initiated to improve the characterization and understanding of these types of deposits and to facilitate and expedite future curatorial responses. The OSL dating programme provides an improved chronological framework for the river terrace and head/brickearth deposits in the study area. The results confirm that most brickearths appear to have formed during the peak of the Last Glacial Maximum around 20,000 BP and may therefore be of lower Palaeolithic potential. However, the OSL dating has also shown that some of the outcrops are considerably older and may therefore hold greater potential for rare Neanderthal or pre-Neanderthal remains.

CONTRIBUTORS
Jean-Luc Schwenninger, Martin Bates, Paul Cuming, Elisabeth Dyson, and Francis Wenban-Smith

ARCHIVE LOCATION
Kent HER, Heritage Conservation, Kent County Council, Invicta House, County Hall, Maidstone, Kent, ME14 1XX

DATE OF RESEARCH
2013–2014

CONTACT DETAILS
Research Laboratory for Archaeology and the History of Art, University of Oxford, Dyson Perrins Building, South Parks Road, Oxford OX1 3Q
Jean-Luc Schwenninger; jean-luc.schwenninger@rlaha.ox.ac.uk.

School of Archaeology, History and Anthropology, University of Wales Trinity Saint David, Lampeter Campus, Ceredigion, SA48 7ED
Martin Bates; m.bates@tsd.ac.uk

Heritage Conservation, Kent County Council, County Hall, Maidstone, ME14 1XX
Paul Cuming; paul.cuming@kent.gov.uk
Elisabeth Dyson; lis.dyson@kent.gov.uk

Faculty of Humanities, University of Southampton, Avenue Campus, Highfield, Southampton, SO17 1BF
Francis Wenban-Smith; F.Wenban-Smith@soton.ac.uk

CONTENTS

Introduction 1

General project background 1

Fieldwork programme and sample collection 1

Methods 3

The physical basis of luminescence dating 3

Sample preparation 4

The single aliquot regenerative-dose (SAR) protocol 6

Measurement procedures and conditions 7

Results and discussion 8

Conclusion 13

References 14

Appendix 1 Details of the OSL dating 16

Appendix 2 Elemental analysis by fusion ICP-MS 21

Appendix 3: Typical OSL shine down curves, growth curves, and D_e distributions 26

© HISTORIC ENGLAND

INTRODUCTION

General project background

The OSL dating programme formed part of a wider research project led by Kent County Council working with financial support from English Heritage. The project was primarily aimed at improving curatorial understanding of the Palaeolithic resources in the Stour Basin area in east Kent (Fig 1), with particular goals of developing a predictive model of areas of high Palaeolithic importance and improving our understanding of brickearth deposits, many of which are located in areas of high development threat and are of uncertain (and possibly high) Palaeolithic potential.

Fieldwork programme and sample collection

The project involved a small fieldwork programme with two main goals: (1) to investigate a detailed transect up the east side of the Blean plateau, to try and provide a more secure dating framework for the terrace and brickearth deposits of the Great Stour in the Canterbury area that have produced rich Palaeolithic remains over the last century; and (2) to investigate brickearth deposits in different parts of the project region, initially to try and establish how and when they were formed. A representative range of brickearthdeposits were selected for test pit investigation in different topographic and geomorphological situations, with a view to developing a model that classifies brickearth outcrops into different types and periods, leading to the possibility of then assessing their Palaeolithic potential. Most brickearthsare thought to have been laid down during the peak of the Last Glacial Maximum *c* 20,000 BP. However, some outcrops are thought to be much older, and therefore may have greater potential for rare Neanderthal or pre-Neanderthal remains. OSL dating is the only dating method available that can be used to date brickearth deposits.

Six sites were identified for more detailed investigations (Fig 1). One aspect of the dating programme was to identify whether the brickearths at these sites typically formed as a single episode, or whether individual outcrops formed over distinct periods of time and may therefore contain much older deposits buried under younger ones.

In the majority of cases, field sampling for OSL dating was carried using light-sealed pvc tubes but in a few cases the compactness or cemented nature of the sediment required the removal of block samples. In all cases, separate double-bagged sediment samples for determining their moisture content were also collected. Where possible, direct measurements of the natural ionizing radiation were obtained using a portable field gamma-ray spectrometer (EG&G

Ortecmicronomad) calibrated against the Oxford blocks (Rhodes and Schwenninger 2007). Sample processing and luminescence measurements were made at the Research Laboratory for Archaeology & the History of Art, University of Oxford. Further details regarding individual samples are presented in Table 1.

Figure 1: Stour Basin Palaeolithic Project – fieldwork sites

Table 1: OSL sample details

Site code	Field code	Laboratory code	OS reference	*In situ* NaI γ-ray spectrometry
CCF13	OSL 02	X6419	TR 22621 65259	Yes
CCF13	OSL 03	X6420	TR 22497 65191	Yes
CCF13	OSL 04	X6421	TR 22497 65191	Yes
CCF13	OSL 05	X6422	TR 22431 65085	Yes
CCF13	OSL 06	X6423	TR 22431 65085	Yes
CCF13	OSL 09	X6424	TR 21784 64186	Yes
CCF13	OSL 10	X6425	TR 21784 64186	Yes
CCF13	OSL 11	X6426	TR 21072 64273	Yes
CCF13	OSL 13	X6427	TR 21072 64273	Yes
CCF13	OSL 15	X6428	TR 22438 64992	Yes
CCF13	OSL 16	X6429	TR 22438 64992	No
CCF13	OSL 17	X6430	TR 22438 64992	Yes
HAF13	OSL 01	X6411	TR 19621 44647	Yes
HAF13	OSL 02	X6412	TR 19621 44647	Yes
HF13	OSL 01	X6418	TQ 92835 48668	Yes
OMF13	OSL 02	X6410	TR 11102 36204	Yes
SOF13	OSL 01	X6414	TR 31585 68757	Yes
SOF13	OSL 02	X6415	TR 31585 68757	Yes
SOF13	OSL 03	X6416	TR 31537 68942	No

Site code	Field code	Laboratory code	OS reference	*In situ* NaI γ-ray spectrometry
SOF13	OSL 04	X6417	TR 31537 68942	No
THL13	OSL 04	X6413	TR 31657 66766	No

METHODS

The physical basis of luminescence dating

When ionising radiation (predominantly alpha, beta or gamma radiation) interacts with an insulating crystal lattice (such as quartz or feldspar), a net redistribution of electronic charge takes place. Electrons are stripped from the outer shells of atoms and though most return immediately, a proportion escape and become trapped at meta-stable sites within the lattice. This charge redistribution continues for the duration of the radiation exposure and the amount of trapped charge is therefore related to both the duration and the intensity of radiation exposure. Even though trapped at meta-stable sites, electrons are 'freed' if the crystal is subjected to heat or exposed to light. Once liberated, a free electron may become trapped once again or may return to a vacant position caused by the absence of a previously displaced electron (a 'hole'). This latter occurrence is termed 'recombination' and the location of the hole is described as the 'recombination centre'. As recombination occurs, a proportion of the energy of the electron is dissipated. Depending upon the nature of the centre where recombination occurs, this energy is expelled as heat and/or light. Therefore, when the crystal (mineral grain) is either heated or illuminated following natural or artificial laboratory irradiation (the 'dose') the total amount of light emitted (luminescence) is directly related to the population of liberated electrons and available number of recombination sites. This is the fundamental principle upon which luminescence dating is based.

In cases where the duration of dosing is not known (as is the case for dating of archaeological sediments), estimates can be made from laboratory measurements. The response (the sensitivity) of the sample to radiation dose (ie the amount of light observed for a given amount of laboratory radiation, usually β-radiation) must be established. From this relationship, the equivalent radiation exposure required to produce the same amount of light as that observed following the natural environmental dose can be determined, and is termed the palaeodose or 'equivalent dose' (D_e). The palaeodose (measured in Gy) is therefore an estimate of the total dose absorbed during the irradiation period (ie burial period). When the dose rate (the amount of radiation per unit time, measured in μGy/a or Gy/ka) is measured (or calculated from measured concentrations of radionuclides), the duration of the dosing period can be calculated using the equation:

Duration of dosing period = Palaeodose ÷ dose rate.

The technique of optical dating was first applied to quartz mineral grains by Huntley *et al* (1985) and a more detailed account of the method may be found in Aitken (1998). Further developmental research has seen the introduction of palaeodose determinations that use the 'single aliquot regenerative-dose' (SAR) measurement protocol (Murray and Wintle 2000) as outlined in more detail in the guidelines published by English Heritage (Duller 2008). These protocols generally have the potential to provide improved accuracy (eg through correction of sensitivity change and interpolation rather than extrapolation of D_e values) as well as increased precision. In some cases they may also provide an indication of incomplete zeroing of the luminescence signal at the time of deposition as detected by the relative dispersal in individual palaeodose estimates or the asymmetry of the D_e distributions.

Sample preparation

The laboratory procedures adopted for the optical dating were based on standard methodologies and designed to yield pure sand sized quartz mineral grains of a defined size range (either 125–180μm or 180–250μm). In order to obtain this material, samples were taken through a preparation procedure which is outlined in more detail below. All laboratory treatments were performed under low intensity laboratory lighting, from purpose-built amber LED lighting (emitting at ~588nm).

After removal of the exposed ends of the tube sampling containers (or the outer 1-2cm layer in the case of the block samples), the unexposed central portion of the sample was wet-sieved to isolate the different constituent mineral size fractions. The preferred grain size was 180–250μm but in the case of samples X6411, X6412 and X6426, the fine texture of the brickearth sediment implied that a smaller grain size range had to be selected (125–180μm) in order to secure sufficient quantities of material for dating. The chosen fractions were treated with diluted hydrochloric acid (HCl) to remove carbonates and then placed in concentrated (48%) hydrofluoric acid for 90 minutes. This latter acid digestion serves two purposes: (i) to dissolve feldspar grains, and (ii) to remove (ie etch) the outer rind of quartz grains (the only part of each quartz grain exposed during burial to natural alpha radiation). Any heavy minerals present were subsequently removed by gravity separation using a sodiumpolytungstate solution at 2.68g.cm^{-3}. Finally, each sample was re-sieved to remove heavily etched smaller grains. The prepared quartz samples were mounted on 9mm diameter aluminium discs for luminescence measurements using viscous silicone oil. Because of suspected partial bleaching problems encountered in samples of fluvial (terrace deposits) rather than aeolian (brickearths) origin, and in some instances because of the small amount of grains available for dating, we

reduced the aliquot size to circa 3mm in order to improve the detection of poorly bleached grains (through the spread and symmetry of individual palaeodose estimates) and thus help to minimize the effects of potential age overestimation.

Various tests for sample purity were made including exposure of grains (within the Risø measurement system) to infrared (IR) light. Quartz generally does not produce measurable IR luminescence at room temperature whereas feldspar, which can suffer from anomalous fading of the infrared stimulated luminescence (IRSL) and OSL signals, or may be less rapidly bleached in some environments, produces an intense luminescence emission when stimulated with infrared light. The presence of a strong IRSL signal is therefore used as an indication for the presence of feldspar contaminants and can be used as a criterion for rejection. In the rare cases where samples are rejected due to presence of high levels of IRSL, the prepared sediment sample can be treated for a prolonged period (two weeks) in concentrated fluorosilicic acid (H_2SiF_6) which effectively dissolves non-quartz material before proceeding to the dating phase (luminescence measurement). In the case of the samples from the Stour Basin, no prolonged etching in H_2SiF_6 was necessary as samples were found to have extremely low IRSL/OSL ratios well below 0.01, (ie IRSL <1% of OSL signal, see Table 3.1). The measurement sequence adopted for providing palaeodose estimates also included a post-IR blue OSL procedure (Banerjee *et al* 2001) designed to deplete any potential feldspar contribution to the OSL signal, by preceding each OSL measurement with an IRSL measurement. The IR exposure reduces the size of feldspathic contributions, besides providing a potential alternative means to determine a palaeodose. In the context of this study, sets of twelve individual aliquots were measured per sample although only a reduced number of six individual measurements could be made for sediment samples containing by low quantities of sand sized mineral material. For some samples two to three additional aliquots were used to conduct dose recovery tests in order to establish whether a known laboratory dose could be recovered following deliberate bleaching of the sample without any prior thermal treatment (contrary to the repeat dose step within the SAR measurement procedure in which aliquots have undergone prior pre-heating and sensitization). Successful recovery of the given dose can be considered to be indicative of an adequate choice of preheat conditions as well as other parameters and instrument settings used for OSL dating.

In order to determine the attenuating effect of pore water on the environmental dose rate of the sediments, additional sediment samples were collected in the field and hermetically sealed. The modern moisture content of such samples was determined in the laboratory by weighing the sample before and after oven drying at 50°C. These determinations formed the basis for the assessment of the mean water content of the samples throughout the burial period and were used in the dose rate calculations (see Table 3.2).

The single aliquot regenerative-dose (SAR) protocol

The SAR method is a regeneration procedure where the light level of the natural signal is converted into Gy via an interpolation between regenerated (ie known dose) points. The natural and regenerated signals are measured using the same aliquot. Sensitivity change commonly observed in quartz TL/OSL dating has previously precluded meaningful results being obtained this way. A key development reported by Murray and Wintle (2000) is that sample (aliquot) sensitivity is monitored following each OSL measurement (Li) using the OSL response to a common test dose (Si). Plots of Li/Si provide the necessary (sensitivity change corrected) data for interpolation. The procedure is further outlined in Figure 2.1.

Steps 1–6 are repeated n times in order to produce the data points required for interpolation (the first dose β1 being zero, to give a measure of the natural signal). Typically n=7 (ie the natural plus 6 regeneration points, including one zero dose point and one repeat point). PH1 and PH2 are usually different although Murray and Wintle (2000) report no dependence of the palaeodose on either (over the range of 200–280°C). The OSL signal is integrated over the initial part of the decay (to ~10% of initial intensity) and the background is taken as the light level measured at the end of each OSL measurement.

Murray and Wintle (2000) have introduced two further steps in to the measurement procedure. The first is the re-measurement of the first regenerated data point (indicated by the box in the explanatory Fig 2). The ratio of the two points (the "recycling ratio") provides an assessment of the efficacy of the sensitivity correction and the accuracy of the technique (large differences being suggestive of an ineffective technique). The recycling ratio (ideally unity) is typically in the range 0.95–1.05. The second additional step is a measurement of the regenerated OSL due to zero dose. This value gives a measure of the degree of thermal transfer to the trap(s) responsible for OSL during pre-heating. The ratio of this value to the natural OSL value (both corrected for sensitivity change) gives the "thermal transfer or recuperation ratio" and ideally this should be in the range of 0.005–0.020.

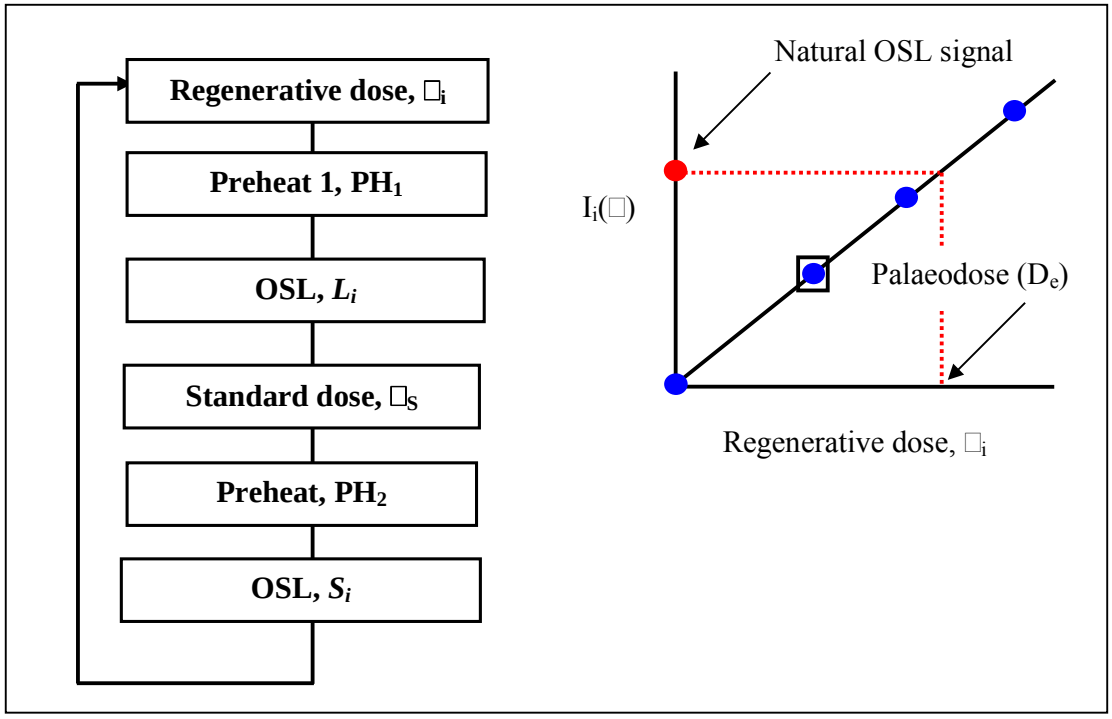

Figure 2: The SAR measurement procedure

Measurement procedures and conditions

Luminescence measurements were made using automated Risø luminescence measurement equipment. Optical excitation for determining the quartz OSL signal intensity was provided by filtered blue diodes (emitting ~410–510nm) and infrared stimulation was provided using an array of IR diodes. Detection of the emitted quartz UV signal (~370 nm) was made using EMI 9635Q bialkali photomultiplier tubes, filtered with Hoya U340 glass filters. Sample irradiation was provided by calibrated sealed 90Sr sources.

All OSL measurements were made at a raised temperature of 125°C (to ensure no re-trapping of charge to the 110°C TL trap during measurement) for 100s. The signal detected in the initial two seconds (with the stable background count rate from the last ten seconds subtracted) was corrected for sensitivity using the OSL signal regenerated by a subsequent beta dose (βs). To ensure removal of unstable OSL components, removal of dose quenching effects, and to stimulate re-trapping and ensure meaningful comparison between naturally and laboratory irradiated signals, pre-heating was performed prior to each OSL measurement.

Following each regenerative dose (βi) and the natural dose, a pre-heat (PH1) at 260°C for 10s was used. Following each test dose (βs), a pre-heat (PH2) of

220°C for 10s was applied. As mentioned previously, all the OSL measurements incorporated a post-IR blue OSL stage in which each OSL measurement is preceded by an IRSL measurement at 50°C, to reduce the potential effects of any residual feldspar grains (Banerjee *et al* 2001) but the SAR procedure is otherwise unchanged. For each sample a typical set of 12 small sized (3–6mm) multigrain aliquots were measured. Before initiating the measurement of the samples from this project, some aliquots were deliberately bleached in natural daylight (15minutes) in order to erase the natural signal. These aliquots were then given a known laboratory dose corresponding to circa 110Gy in order to obtain a recovered dose. The results of this dose recovery test showed that the recovered dose was within 5% of the given laboratory dose thereby confirming that the adopted preheats, measurement procedures and instrument settings were suited to the dating of these samples.

RESULTS AND DISCUSSION

A summary of the luminescence characteristics is presented in Table 3 and the results of the OSL measurements, radioactivity data and age estimates are presented in Table 4. More detailed information pertaining to age calculations and geochemical composition of individual samples are provided in Appendices 1 and 2. Typical OSL signal plots, growth curves and palaeodose distributions can be found in Appendix 3. The yield of sand sized quartz mineral grains derived from the samples was generally sufficient and the prepared aliquots also showed good response to laboratory irradiation (sensitivity). The initial signal intensity and the form of the decay curve show a fast decrease in OSL intensity which is characteristic of quartz (Appendix 3). This is further evidenced by a well defined 110°C TL peak and stimulation using infrared (IR) laser diodes also confirmed the purity of each aliquot with absolutely negligible contributions from potential feldspathic contaminants (<0.1%; see IRSL/OSL ratio in Table 3). In the SAR measurements a low irradiation dose was repeated (recycling point) at the end of the measurement cycle to test how well the SAR sensitivity correction procedure was working. If the sensitivity correction is adequate then the ratio of the signal from the repeated dose to that of the initial regeneration dose should fall within the range of 0.9–1.10. Excellent recycling ratios close to unity were recorded for all the samples analysed in this study. A further test on the recuperation (thermal transfer) also showed that no significant recuperation of the OSL signal was detected in the large majority of aliquots. Dose response curves generally pass through the origin when a 'zero' Gy beta dose is included thus indicating that thermal transfer of charge from optically insensitive traps into OSL traps is not a problem.

With the exception of sample X6423 (CCF-OSL06) the concentrations of radioisotopes (K, Th, and U) are generally elevated (see Table 4). The fine textured nature of the silty brickearth deposits favours a high dose environment suitable for the dating of relatively young samples below 100ka. However, the

reverse is generally true for older deposits. Dose rates in excess of 2.5Gy/ka are likely to lead to an early onset of the OSL signal saturation thereby making it more difficult to determine an accurate age for older deposits in excess of 100ka. Minimum age estimates may be obtained for fully saturated samples but for samples found to be close to saturation as well as being additionally characterized by poor bleaching, the dating may become more problematic and unreliable. The majority of samples analysed here are below saturation levels but in the case of some samples (ie X6411, X6412) the measurements did reveal the presence of saturated aliquots. This may have been caused by the presence of grains having retained a strong residual signal as a result of poor bleaching during deposition. The latter were rejected from the analysis but due to the limited number of individual OSL measurements which could be made (only six for each of these samples) as a result of the paucity of quartz mineral grains available for dating, the calculated age estimate is strongly dependent on the small number of palaeodose determinations (ie only four in each case). Although, these dates may be considered to be less reliable, the increased uncertainty should be reflected in the inflated errors associated with the dates obtained for both samples. Furthermore, the presumed aeolian origin of the brickearth deposits analysed in this study should reduce the potential negative effects of poor bleaching commonly associated with fluvial sediments. Although, it is not impossible that some brickearths may have been reworked by fluvial processes or affected by post depositional bioturbation or even simply deposited at night, it is unlikely that the OSL measurements can be considered to have been seriously compromised by partial bleaching issues. Some of the samples collected close to the top of the stratigraphic sequence and which have provided surprisingly young dates may indeed have experienced some degree of mixing of their grain population through soil formation processes including bioturbation (ie earthworm activity). Samples X6414, X6415 and X6430 for instance were collected from depths of only 25cm, 45cm, and 35cm below the surface and the distribution of individual palaeodose estimates (especially in the case of the former two samples) may be considered as being widely distributed with individual D_e values ranging from ~1 to 12 Gy (see Appendix 3). However, despite the low precision (10–30%) obtained for the dating of these samples, the results unquestionable hint at a Late Holocene age for the deposition or reworking of these sediments as opposed to a Devensian or Early Holocene origin. This finding is rather unexpected and would merit further sedimentological investigation.

Table 3: Summary of luminescence characteristics including tests for recycling, recuperation, feldspar contamination as well as a qualitative assessment of sensitivity and signal saturation

Sample code	Mean Recycling ratio	Recuperation	Mean IRSL/OSL ratio	Sensitivity	Signal saturation
X6410	1.00	1.07	0.001	Very good	No
X6411	1.00	0.08	0.001	Very good	No (except 2)
X6412	0.98	0.18	0.002	Very good	No (except 2)
X6413	1.02	1.08	0.001	Very good	No
X6414	1.03	3.52	0.001	Very good	No
X6415	1.05	5.13	0.003	Very good	No
X6416	1.02	0.31	0.014	Very good	No
X6417	0.99	0.32	0.013	Very good	No
X6418	1.01	1.68	0.005	Very good	No
X6419	0.99	1.09	0.001	Very good	No
X6420	1.01	-	0.004	Very good	No
X6421	1.00	-	0.002	Very good	No
X6422	1.00	0.78	0.001	Very good	No
X6423	0.98	0.68	0.002	Very good	No
X6424	1.03	1.67	0.002	Very good	No
X6425	0.96	0.48	0.002	Very good	No
X6426	1.01	0.78	0.001	Very good	No
X6427	1.01	1.45	0.002	Very good	No
X6428	0.96	0.38	0.002	Very good	No
X6429	-	-	0.002	Very good	No
X6430	-	-	0.001	Very good	No

As mentioned above, sample X6423 was characterized by a very low dose rate of only 0.58Gy/ka (see Table 4). This is substantially less than any of the other samples in the series which have a mean dose rate of 2.53Gy/ka. The concentrations of all three radionuclides (K, Th and U) are considerably lower for this sample (see Table 4) and this could raise suspicion on to the integrity of the dosimetric analysis. A much reduced dose rate has a massive effect on the age determination and indeed, if the recorded dose rate of this sample had been similar to that obtained for the other samples then the age estimate of 247ka would have been reduced to only circa 57ka. However, the full elemental composition (see Appendix 2) reveals that the chemical composition of this sample is very different from all the others in the series. This strongly suggests that the measured concentrations of radioisotopes are genuine and unlikely to have been caused by a fault during the analysis thus lending support to the obtained results. This sample provided the oldest date in the series and the result is not unexpected. In a similar way, samples X6411, X6412, X6425 and X6428 which are also deep-lying also provided older age estimates of respectively 143ka, 120ka, 143ka and 137ka. These results should not to be regarded as minimum age estimates and despite the limited number of palaeodose measurements available for analysis as well as the relatively large error attached to most of these results, the latter should provide a good

indication of the true antiquity of the sediment. Sample X6411 provided an older date than the underlying sample X6412 but it is important to note that the palaeodose determinations remain within error. Furthermore, in the case of sample X6412 a single low outlying measurement (see Appendix 3) is causing the D_e dose distribution to be skewed towards the lower values. Without this 'outlier' the mean palaeodose distribution would be in much better agreement with the mean D_e value obtained from the overlying sample X6411.

More generally, the OSL dating seems to clearly indicate the predominance of accumulation of brickearth deposits around the time of the Last Glacial Maximum under extremely cold and dry, peri- or postglacial conditions. This finding is in good agreement with the expectations for the timing of these superficial windblown deposits sometimes described as periglacial loess. Some of the dating results could hint at the existence of multiple phases of deposition (ie results of *c* 20ka and 27ka obtained for samples X6426 and X6427) but unfortunately, the resolution of the OSL dating cannot be considered to be sufficiently good to support such a claim. However, one of the samples (X6413) provided a significantly younger date of circa 13ka. This Late Devensian age was unexpected and is particularly interesting as it may relate to deposition or reworking during the Younger Dryas (12800–11500 BP), a period which saw the abrupt return to dry and cold climatic conditions

Table 4: Summary of the OSL dating. The results are based on luminescence measurements of sand-sized quartz grains (90–125 or 180–255μm) mounted on small 3–4mm sized aliquots. All samples were measured in automated Risø luminescence readers (Bøtter-Jensen, 1988, 1997, 2000) using a SAR post-IR blue OSL measurement protocol (Murray and Wintle 2000, Banerjee et al *2001, Wintle and Murray 2006). Dose rate calculations are based on the concentration of radioactive elements (potassium, thorium and uranium) derived from elemental analysis by ICP-MS/AES using a fusion sample preparation technique. The final OSL age estimates include an additional 2% systematic error to account for uncertainties in source calibration. Dose rate calculations are based on Aitken (1985). These incorporated beta attenuation factors (Mejdahl 1979), dose rate conversion factors (Adamiec and Aitken 1998) and an absorption coefficient for the water content (Zimmerman 1971). The contribution of cosmic radiation to the total dose rate was calculated as a function of latitude, altitude, burial depth and average over-burden density based on data by Prescott and Hutton (1994). Further details pertaining to individual samples are presented in Appendix 1*

		Radioisotopes †			Field Water (%)	External γ-dose rate§ (Gy/ka)	Cosmic dose rate (Gy/ka)	Total dose rate (Gy/ka)	Palaeodose♦(Gy)	OSL date (ka)
Field code	Lab. code	K (%)	Th(ppm)	U (ppm)						
CCF/02	X6419	1.56	8.9	2.5	13.9	0.916 ± 0.021	0.170 ± 0.013	2.44 ± 0.17	50.18 ± 3.63	20.58 ± 2.06
CCF/03	X6420	1.49	8.9	2.6	10.8	0.948 ± 0.021	0.166 ± 0.013	2.49 ± 0.17	50.60 ± 2.97	20.30 ± 1.84
CCF/04	X6421	1.58	8.2	2.4	13.8	0.882 ± 0.021	0.158 ± 0.012	2.38 ± 0.16	48.20 ± 6.50	20.26 ± 3.08
CCF/05	X6422	1.86	10.8	2.7	6.0	1.129 ± 0.018	0.169 ± 0.013	2.97 ± 0.16	55.01 ± 6.12	18.50 ± 2.32
CCF/06	X6423	0.31	1.4	0.4	4.0	0.166 ± 0.028	0.153 ± 0.012	0.58 ± 0.03	143.94 ± 16.01	*246.94 ± 30.04*
CCF/09	X6424	1.53	7.8	2.3	8.4	0.912 ± 0.028	0.181 ± 0.015	2.50 ± 0.14	48.77 ± 8.56	19.54 ± 3.59
CCF/10	X6425	1.00	7.4	2.0	11.7	0.710 ± 0.029	0.165 ± 0.013	1.84 ± 0.12	*262.15 ± 81.54*	*142.69 ± 45.38*
CCF/11	X6426	1.61	7.9	2.4	9.5	0.922 ± 0.027	0.161 ± 0.012	2.56 ± 0.14	51.17 ± 7.95	20.03 ± 3.30
CCF/13	X6427	0.84	5.0	1.4	7.6	0.546 ± 0.024	0.152 ± 0.011	1.50 ± 0.08	40.05 ± 5.02	26.74 ± 3.63
CCF/15	X6428	1.22	6.2	1.9	4.0	0.761 ± 0.024	0.139 ± 0.010	2.07 ± 0.11	*284.34 ± 69.03*	*137.22 ± 34.15*
CCF/16	X6429	1.76	10.9	2.9	21.8	0.965 ± 0.021	0.173 ± 0.014	2.52 ± 0.17	58.74 ± 3.56	23.35 ± 2.13
CCF/17	X6430	1.68	10.4	2.9	4.1	1.163 ± 0.021	0.193 ± 0.020	3.04 ± 0.16	6.20 ± 1.2	2.04 ± 0.41
HAF/01	X6411	1.49	13.2	2.9	18.4	1.054 ± 0.021	0.174 ± 0.014	2.61 ± 0.17	*374.50 ± 56.59*	143.25 ± 23.65
HAF/02	X6412	1.54	11.7	2.8	20.1	0.972 ± 0.021	0.157 ± 0.012	2.47 ± 0.17	*296.56 ± 41.42*	119.91 ± 18.61
HF/01	X6418	1.42	8.8	2.4	11.7	0.896 ± 0.021	0.187 ± 0.016	2.37 ± 0.12	44.73 ± 3.55	18.84 ± 1.79
OMF/02	X6410	1.72	10.7	3.0	17.5	1.027 ± 0.021	0.169 ± 0.013	2.66 ± 0.18	51.63 ± 4.75	19.36 ± 2.23
SOF/01	X6414	1.44	8.5	2.4	9.2	0.923 ± 0.021	0.194 ± 0.021	2.47 ± 0.13	2.56 ± 0.35	1.04 ± 0.15
SOF/02	X6415	1.46	8.8	2.5	9.7	0.938 ± 0.021	0.189 ± 0.018	2.49 ± 0.13	1.96 ± 0.65	0.79 ± 0.26
SOF/03	X6416	0.87	6.5	1.5	9.5	0.613 ± 0.021	0.193 ± 0.020	1.64 ± 0.08	27.58 ± 2.63	16.77 ± 1.80
SOF/04	X6417	1.15	6.3	1.9	11.7	0.704 ± 0.021	0.167 ± 0.013	1.92 ± 0.10	40.34 ± 6.04	20.98 ± 3.33
THL/04	X6413	1.20	9.3	2.1	13.2	0.831 ± 0.021	0.185 ± 0.016	2.14 ± 0.14	27.09 ± 1.47	12.68 ± 1.09

† Measurements were made on dried, homogenised and powdered material by fusion ICP-MS with an assigned systematic uncertainty of ±5%. Dry beta dose rates calculated from these activities were adjusted for the measured field water content expressed as a percentage of the dry mass of the sample.

§ Based on *in-situ* measurements using a portable γ-ray spectrometer equipped with a 3x3 inch NaI (Tl) scintillator crystal and calibrated against the Oxford calibration blocks (Rhodes and Schwenninger 2007). For samples X6413, X6416, X6417 and X6429 the external dose rate was calculated from the concentrations of radioisotopes determined by fusion ICP-MS.

♦ Values highlighted in italics are problematic mainly as a result of suspected partial bleaching and consequently, the calculated age estimates inserted in brackets are considered to be unreliable.

CONCLUSION

With the exception of samples (X6414, X6415, and X6430) the results of the OSL dating programme show that the samples are predominantly of expected Pleistocene age. These Late Holocene age estimates may represent recent reworking of older brickearth deposits. However, the majority of the OSL dates are clustered around 20ka and these findings confirm that most brickearths in the study area have formed during the peak of the Last Glacial Maximum (LGM) around 20,000 BP and may therefore be of lower Palaeolithic potential. Some of the age determinations also suggest that some of the outcrops might be considerably older and may therefore hold greater potential for rare Neanderthal or pre-Neanderthal remains. From a planning perspective, these deposits may in future merit closer curatorial attention.

REFERENCES

Adamiec, G, and Aitken, M J, 1998 Dose-rate conversion factors: update, *Ancient TL*, **16**, 37–50

Aitken Aitken, M J, 1998 *Introduction to optical dating*, Oxford: Oxford University Press

Banerjee, D, Murray, A S, Bøtter-Jensen, L, and Lang, A, 2001 Equivalent dose estimation using a single aliquot of polymineral fine grains, *Radiation Measurements*, **33**, 73–94

Bøtter-Jensen, L, 1988 The automated Riso TL dating reader system,*Nuclear Tracks and Radiation Measurements*, **14**, 177–80

Bøtter-Jensen, L, 1997 Luminescence techniques: instrumentation and methods, *Radiation Measurements*, 27, 749–68

Bøtter-Jensen, L, Bulur, E, Duller, G A T, Murray, A S, 2000 Advances in luminescence instrument systems, *Radiation Measurements*, **32**, 523–28

Duller, G A T, 2008 *Luminescence Dating: Guidelines on using luminescence dating in archaeology*, English Heritage: Swindon

Huntley, D J, Godfrey-Smith, D I, and Thewalt, M L W, 1985 Optical dating of sediments, *Nature*, **313**, 105–7

Mejdahl, V, 1979 Thermoluminescence dating: beta dose attenuation in quartz grains, *Archaeometry*, **21**, 61–73

Murray, A S, and Wintle, A G, 2000 Luminescence dating of quartz using an improved single-aliquot regenerative-dose protocol, *Radiation Measurements*, **32**, 57–73

Prescott, J R, and Hutton, J T, 1994 Cosmic ray contributions to dose rates for luminescence and ESR dating: large depths and long term time variations, *Radiation Measurements*, 23, 497–500

Rhodes, E J, and Schwenninger, J-L, 2007 Dose rates and radioisotope concentrations in the concrete calibration blocks at Oxford, *Ancient TL*, **25**, 5–8

Wintle, A G, and Murray, A S, 2006 A review of quartz optically stimulated luminescence characteristics and their relevance in single-aliquot regeneration dating protocols, *Radiation Measurements*, **41**, 369–91

Zimmermann, D W, 1971 Thermoluminescent dating using fine grains from pottery, *Archaeometry*, **13**, 29–52

APPENDIX 1 DETAILS OF THE OSL DATING

Client code	OMF13-02	HAF13-01	HAF13-02	THL13-04
Laboratory code	X6410	X6411	X6412	X6413
D_e (Gy)	51.63	374.50	296.56	27.09
Total uncertainty	4.75	56.50	41.42	1.47
Measured uncertainty (includes 2% instrument error)	4.64	56.00	40.99	1.37
Additional calibration error 2%	1.03	7.49	5.93	0.54
Grain size				
Min. grain size (mm)	180	125	125	180
Max grain size (mm)	255	180	180	255
External gamma dose rate available (Y/N)	Yes	Yes	Yes	No
External gamma dose rate (Gy/ka)	1.027	1.054	0.972	0.831
Error	0.051	0.053	0.049	0.042
Measured concentrations	ICP-MS	ICP-MS	ICP-MS	ICP-MS
Standard fractional error	0.050	0.050	0.050	0.050
% K	1.718	1.486	1.544	1.204
Error (%K)	0.086	0.074	0.077	0.060
Th (ppm)	10.700	13.200	11.700	9.300
Error (ppm)	0.535	0.660	0.585	0.465
U (ppm)	3.000	2.900	2.800	2.100
Error (ppm)	0.150	0.145	0.140	0.105
Cosmic dose calculations				
Depth (m)	1.65	1.65	2.42	1.18
Error (m)	0.05	0.05	0.05	0.05
Average overburden density (g.cm^3)	1.90	1.90	1.90	1.90
Error (g.cm^3)	0.10	0.10	0.10	0.10
Latitude (deg.), north positive	51.00	51.00	51.00	51.00
Longitude (deg.), east positive	1.00	1.00	1.00	1.00
Altitude (m above sea-level))	1.65	141.88	141.11	150.00
Geomagnetic latitude	53.564	53.564	53.564	53.564
Dc (Gy/ka), 55N G.lat, 0 km Alt.	0.169	0.169	0.153	0.180
Error	0.013	0.013	0.012	0.015
Cosmic dose rate (Gy/ka)	0.169	0.174	0.157	0.185
Error	0.013	0.014	0.012	0.016
Moisture content				
Measured water in tubes (% of wet sediment)	17.50	18.36	20.12	13.16
Moisture (water / wet sediment)	0.17	0.18	0.20	0.13
Error	0.05	0.05	0.05	0.05
Total dose rate, Gy/ka	2.662	2.614	2.473	2.136
Error	0.183	0.175	0.167	0.142
% Error	6.859	6.704	6.768	6.665
AGE (ka)	19.40	143.25	119.91	12.68
Error	2.23	23.65	18.61	1.09

APPENDIX 1 (CONTINUED) DETAILS OF THE OSL DATING

Client code	SOF13-01	SOF13-02	SOF13-03	SOF13-04
Laboratory code	X6414	X6415	X6416	X6417
D_e (Gy)	2.56	1.96	27.58	40.34
Total uncertainty	0.35	0.65	2.63	6.04
Measured uncertainty (includes 2% instrument error)	0.35	0.65	2.57	5.99
Additional calibration error 2%	0.05	0.04	0.55	0.81
Grain size				
Min. grain size (mm)	180	180	180	180
Max grain size (mm)	255	255	255	255
External gamma dose rate available (Y/N)	Yes	Yes	No	No
External gamma dose rate (Gy/ka)	0.923	0.938		
Error	0.046	0.047		
Measured concentrations	ICP-MS	ICP-MS	ICP-MS	ICP-MS
Standard fractional error	0.050	0.050	0.050	0.050
% K	1.444	1.461	0.872	1.146
Error (%K)	0.072	0.073	0.044	0.057
Th (ppm)	8.500	8.800	6.500	6.300
Error (ppm)	0.425	0.440	0.325	0.315
U (ppm)	2.400	2.500	1.500	1.900
Error (ppm)	0.120	0.125	0.075	0.095
Cosmic dose calculations				
Depth (m)	0.60	0.80	0.65	1.75
Error (m)	0.05	0.05	0.05	0.05
Average overburden density (g.cm^3)	1.90	1.90	1.90	1.90
Error (g.cm^3)	0.10	0.10	0.10	0.10
Latitude (deg.), north positive	51.00	51.00	51.00	51.00
Longitude (deg.), east positive	1.00	1.00	1.00	1.00
Altitude (m above sea-level))	0.60	0.80	0.65	1.75
Geomagnetic latitude	53.564	53.564	53.564	53.564
Dc (Gy/ka), 55N G.lat, 0 km Alt.	0.194	0.189	0.193	0.167
Error	0.021	0.018	0.020	0.013
Cosmic dose rate (Gy/ka)	0.194	0.189	0.193	0.167
Error	0.021	0.018	0.020	0.013
Moisture content				
Measured water in tubes (% of wet sediment)	9.19	9.71	9.55	9.90
Moisture (water / wet sediment)	0.09	0.10	0.10	0.10
Error	0.03	0.03	0.03	0.03
Total dose rate, Gy/ka	2.472	2.491	1.644	1.922
error	0.131	0.132	0.082	0.101
% error	5.293	5.281	4.972	5.272
AGE (ka)	1.04	0.79	16.78	20.98
Error	0.15	0.26	1.80	3.33

APPENDIX 1 (CONTINUED) DETAILS OF THE OSL DATING

Client code	HF13-01	CCF13-02	CCF13-03	CCF13-04
Laboratory code	X6418	X6419	X6420	X6421
D_e (Gy)	44.73	50.18	50.60	48.20
Total uncertainty	3.55	3.63	2.97	6.50
Measured uncertainty (includes 2% instrument error)	3.44	3.49	2.79	6.43
Additional calibration error 2%	0.89	1.00	1.01	0.96
Grain size				
Min. grain size (mm)	180	180	180	180
Max grain size (mm)	255	255	255	255
External gamma dose rate available (Y/N)	Yes	Yes	Yes	Yes
External gamma dose rate (Gy/ka)	0.896	0.916	0.948	0.882
Error	0.045	0.046	0.047	0.044
Measured concentrations	ICP-MS	ICP-MS	ICP-MS	ICP-MS
Standard fractional error	0.050	0.050	0.050	0.050
% K	1.420	1.561	1.494	1.577
Error (%K)	0.071	0.078	0.075	0.079
Th (ppm)	8.800	8.900	8.900	8.200
Error (ppm)	0.440	0.445	0.445	0.410
U (ppm)	2.400	2.500	2.600	2.400
Error (ppm)	0.120	0.125	0.130	0.120
Cosmic dose calculations				
Depth (m)	1.00	1.60	1.80	2.20
Error (m)	0.05	0.05	0.05	0.05
Average overburden density (g.cm^3)	1.90	1.90	1.90	1.90
Error (g.cm^3)	0.10	0.10	0.10	0.10
Latitude (deg.), north positive	51.00	51.00	51.00	51.00
Longitude (deg.), east positive	1.00	1.00	1.00	1.00
Altitude (m above sea-level))	76.80	1.25	3.92	3.52
Geomagnetic latitude	53.564	53.564	53.564	53.564
Dc (Gy/ka), 55N G.lat, 0 km Alt.	0.184	0.170	0.166	0.157
Error	0.016	0.013	0.013	0.012
Cosmic dose rate (Gy/ka)	0.187	0.170	0.166	0.158
Error	0.016	0.013	0.013	0.012
Moisture content				
Measured water in tubes (% of wet sediment)	11.75	13.91	10.81	13.79
Moisture (water / wet sediment)	0.12	0.14	0.11	0.14
Error	0.03	0.05	0.05	0.05
Total dose rate, Gy/ka	2.374	2.438	2.492	2.379
Error	0.125	0.168	0.172	0.166
% error	5.250	6.900	6.909	6.976
AGE (ka)	18.85	20.58	20.30	20.26
Error	1.79	2.06	1.84	3.08

APPENDIX 1 (CONTINUED) DETAILS OF THE OSL DATING

Client code	CCF13-05	CCF13-06	CCF13-09	CCF13-10
Laboratory code	X6422	X6423	X6424	X6425
D_e (Gy)	55.01	143.94	48.77	262.15
Total uncertainty	6.22	16.27	8.57	81.55
Measured uncertainty (includes 2% instrument error)	6.12	16.01	8.51	81.38
Additional calibration error 2%	1.10	2.88	0.98	5.24
Grain size				
Min. grain size (mm)	180	180	180	180
Max grain size (mm)	255	255	255	255
External gamma dose rate available (Y/N)	Yes	Yes	Yes	Yes
External gamma dose rate (Gy/ka)	1.129	0.166	0.912	0.710
error	0.056	0.008	0.046	0.036
Measured concentrations	ICP-MS	ICP-MS	ICP-MS	ICP-MS
Standard fractional error	0.050	0.050	0.050	0.050
% K	1.860	0.307	1.527	0.996
Error (%K)	0.093	0.015	0.076	0.050
Th (ppm)	10.800	1.400	7.800	7.400
Error (ppm)	0.540	0.070	0.390	0.370
U (ppm)	2.700	0.400	2.300	2.000
Error (ppm)	0.135	0.020	0.115	0.100
Cosmic dose calculations				
Depth (m)	1.65	2.45	1.15	1.85
Error (m)	0.05	0.05	0.05	0.05
Average overburden density (g.cm^3)	1.90	1.90	1.90	1.90
Error (g.cm^3)	0.10	0.10	0.10	0.10
Latitude (deg.), north positive	51.00	51.00	51.00	51.00
Longitude (deg.), east positive	1.00	1.00	1.00	1.00
Altitude (m above sea-level))	6.87	6.07	19.59	18.89
Geomagnetic latitude	53.564	53.564	53.564	53.564
Dc (Gy/ka), 55N G.lat, 0 km Alt.	0.169	0.153	0.180	0.165
Error	0.013	0.012	0.015	0.013
Cosmic dose rate (Gy/ka)	0.169	0.153	0.181	0.165
Error	0.013	0.012	0.015	0.013
Moisture content				
Measured water in tubes (% of wet sediment)	5.97	4.04	8.42	11.70
Moisture (water / wet sediment)	0.10	0.10	0.08	0.12
Error	0.03	0.03	0.03	0.05
Total dose rate, Gy/ka	2.974	0.583	2.496	1.837
Error	0.163	0.026	0.136	0.122
% error	5.476	4.507	5.436	6.621
AGE (ka)	18.50	246.94	19.54	142.69
Error	2.32	30.04	3.59	45.38

APPENDIX 1 (CONTINUED) DETAILS OF THE OSL DATING

Client code	CCF13-15	CCF13-16	CCF13-17	CCF13-13	CCF13-11
Laboratory code	X6426	X6427	X6428	X6429	X6430
D_e (Gy)	51.17	40.05	284.34	58.74	6.20
Total uncertainty	7.96	5.02	69.03	3.56	1.21
Measured uncertainty (includes 2% instrument error)	7.89	4.96	68.80	3.36	1.20
Additional calibration error 2%	1.02	0.80	5.69	1.17	0.12
Grain size					
Min. grain size (mm)	125	180	180	180	180
Max grain size (mm)	180	255	255	255	255
External gamma dose rate available (Y/N)	Yes	No	Yes	Yes	Yes
External gamma dose rate (Gy/ka)	0.922		0.761	0.965	1.163
Error	0.046		0.038		
Measured concentrations	ICP-MS	ICP-MS	ICP-MS	ICP-MS	ICP-MS
Standard fractional error	0.050	0.050	0.050	0.050	0.050
% K	1.610	0.838	1.220	1.760	1.685
Error (%K)	0.081	0.042	0.061	0.088	0.084
Th (ppm)	7.900	5.000	6.200	10.900	10.400
Error (ppm)	0.395	0.250	0.310	0.545	0.520
U (ppm)	2.400	1.400	1.900	2.900	2.900
Error (ppm)	0.120	0.070	0.095	0.145	0.145
Cosmic dose calculations					
Depth (m)	2.05	2.47	3.22	1.48	0.68
Error (m)	0.05	0.05	0.05	0.05	0.05
Average overburden density (g.cm^3)	1.90	1.90	1.90	1.90	1.90
Error (g.cm^3)	0.10	0.10	0.10	0.10	0.10
Latitude (deg.), north positive	51.00	51.00	51.00	51.00	51.00
Longitude (deg.), east positive	1.00	1.00	1.00	1.00	1.00
Altitude (m above sea-level))	8.71	8.29	7.54	23.48	24.28
Geomagnetic latitude	53.564	53.564	53.564	53.564	53.564
Dc (Gy/ka), 55N G.lat, 0 km Alt.	0.160	0.152	0.139	0.173	0.192
Error	0.012	0.011	0.010	0.014	0.020
Cosmic dose rate (Gy/ka)	0.161	0.152	0.139	0.173	0.193
Error	0.012	0.011	0.010	0.014	0.020
Moisture content					
Measured water in tubes (% of wet sediment)	9.54	7.59	4.00	21.76	4.12
Moisture (water / wet sediment)	0.10	0.08	0.05	0.22	0.05
Error	0.03	0.03	0.03	0.05	0.03
Total dose rate, Gy/ka	2.555	1.498	2.072	2.516	3.044
Error	0.141	0.077	0.113	0.171	0.163
% error	5.516	5.165	5.472	6.795	5.364
AGE (ka)	20.03	26.74	137.22	23.35	2.04
Error	3.30	3.63	34.15	2.13	0.41

© HISTORIC ENGLAND

APPENDIX 2 ELEMENTAL ANALYSIS BY FUSION ICP-MS

Analyte Symbol		SiO_2	Al_2O_3	$Fe_2O_3(T)$	MnO	MgO	CaO	Na_2O	K_2O	TiO_2	P_2O_5	LOI	Total
Unit Symbol		%	%	%	%	%	%	%	%	%	%	%	%
Detection Limit		0.01	0.01	0.01	0.001	0.01	0.01	0.01	0.01	0.001	0.01		0.01
Field code	Lab code												
OMF13-02	X6410	77.28	9.69	4.61	0.096	0.78	0.44	0.78	2.07	0.797	0.11	3.66	100.3
HAF13-0	X6411	73.76	11.59	4.93	0.022	0.59	0.35	0.2	1.79	0.923	0.08	5.1	99.33
HAF13-02	X6412	77.38	10.28	4.05	0.032	0.5	0.27	0.23	1.86	0.954	0.08	4.13	99.77
THL13-04	X6413	77.39	8.57	4.79	0.075	0.77	1.01	0.5	1.45	0.579	0.07	4.7	99.92
SOF13-01	X6414	78.85	6.96	2.73	0.068	0.44	2.49	0.83	1.74	0.701	0.09	4.76	99.65
SOF13-02	X6415	79.36	7.02	2.61	0.069	0.41	1.46	0.91	1.76	0.714	0.09	3.93	98.33
SOF13-03	X6416	83.41	6.11	4.17	0.055	0.56	0.77	0.26	1.05	0.445	0.06	3.87	100.8
SOF13-04	X6417	67.87	5.75	3.17	0.043	0.58	9.93	0.51	1.38	0.541	0.08	9.95	99.81
HF13-01	X6418	81.14	8.1	4.21	0.046	0.59	0.44	0.6	1.71	0.624	0.07	3.37	100.9
CCF13-02	X6419	62.7	8.12	3.62	0.051	1.58	9.78	0.78	1.88	0.666	0.12	11.12	100.4
CCF13-03	X6420	62.93	7.62	3.28	0.055	1.67	10.41	0.83	1.8	0.651	0.12	11.32	100.7
CCF13-04	X6421	62.15	7.94	3.27	0.059	1.85	10.4	0.89	1.9	0.624	0.12	11.45	100.6
CCF13-05	X6422	74.58	10.4	4.87	0.074	0.93	0.73	0.88	2.24	0.769	0.11	4.52	100.1
CCF13-06	X6423	96.59	1.38	1.45	0.01	0.11	0.14	0.09	0.37	0.101	0.02	0.67	100.9
CCF13-09	X6424	63.57	7.75	3.1	0.057	1.63	10.07	0.86	1.84	0.58	0.11	10.82	100.4
CCF13-10	X6425	77.6	6.25	4.72	0.062	0.55	3.46	0.35	1.2	0.573	0.05	5.37	100.2
CCF13-11	X6426	64.57	7.75	3.09	0.06	1.63	9.3	0.87	1.94	0.565	0.11	10.21	100.1
CCF13-13	X6427	75.13	4.63	2.48	0.024	0.42	8.17	0.23	1.01	0.462	0.06	8.25	100.9
CCF13-15	X6428	72.44	6.2	3.46	0.044	1	6.71	0.46	1.47	0.524	0.09	7.66	100
CCF13-16	X6429	75.94	10.2	4.53	0.059	0.87	0.96	0.88	2.12	0.751	0.11	4.02	100.4
CCF13-17	X6430	79.75	8.45	3.12	0.091	0.5	0.78	0.9	2.03	0.808	0.07	3.44	99.94

© HISTORIC ENGLAND

APPENDIX 2 (CONTINUED) ELEMENTAL ANALYSIS BY FUSION ICP-MS

Analyte Symbol		Sc	Be	V	Ba	Sr	Y	Zr	Cr	Co	Ni	Cu	Zn
Unit Symbol		ppm	ppm	ppm	ppm	ppm	ppm	ppm	ppm	ppm	ppm	ppm	ppm
Detection Limit		1	1	5	3	2	2	4	20	1	20	10	30
Field cod	Lab code												
OMF13-02	X6410	10	2	87	362	76	35	468	100	15	30	20	60
HAF13-01	X6411	13	2	99	319	48	38	536	100	6	30	20	50
HAF13-02	X6412	13	2	85	345	47	38	597	90	8	20	20	50
THL13-04	X6413	10	2	89	291	76	37	415	90	17	40	20	60
SOF13-01	X6414	6	1	54	353	100	26	522	70	8	<20	20	40
SOF13-02	X6415	6	1	53	365	92	25	516	70	8	<20	<10	30
SOF13-03	X6416	8	2	73	214	59	23	511	90	11	30	10	190
SOF13-04	X6417	7	1	66	236	214	23	375	90	8	20	10	40
HF13-01	X6418	8	2	74	301	61	26	404	90	9	< 20	20	60
CCF13-02	X6419	8	1	72	313	183	25	416	80	9	30	20	50
CCF13-03	X6420	8	1	67	319	178	27	492	80	8	20	10	40
CCF13-04	X6421	8	1	65	338	182	25	385	70	8	20	10	40
CCF13-05	X6422	11	2	93	396	88	34	431	100	12	40	20	60
CCF13-06	X6423	2	<1	22	81	14	5	54	<20	3	<20	<10	<30
CCF13-09	X6424	7	1	64	333	179	23	373	80	8	20	10	40
CCF13-10	X6425	7	1	74	240	65	25	464	90	13	30	20	40
CCF13-11	X6426	7	1	64	334	177	24	374	80	8	20	10	40
CCF13-13	X6427	5	1	53	187	117	16	361	70	6	< 20	<10	30
CCF13-15	X6428	7	1	71	253	130	20	468	90	11	20	20	40
CCF13-16	X6429	10	2	91	373	92	31	465	110	11	40	20	70
CCF13-17	X6430	8	1	65	392	88	27	568	90	9	< 20	10	50

© HISTORIC ENGLAND

APPENDIX 2 (CONTINUED) ELEMENTAL ANALYSIS BY FUSION ICP-MS

Analyte Symbol		Ga	Ge	As	Rb	Nb	Mo	Ag	In	Sn	Sb	Cs	La
Unit Symbol		ppm	ppm	ppm	ppm	ppm	ppm	ppm	ppm	ppm	ppm	ppm	ppm
Detection Limit		1	1	5	2	1	2	0.5	0.2	1	0.5	0.5	0.1
Field code	Lab code												
OMF13-02	X6410	12	2	15	84	14	<2	3.8	<0.2	2	0.7	4.4	39
HAF13-01	X6411	15	2	15	91	15	<2	4.4	<0.2	2	0.8	5.1	43.1
HAF13-02	X6412	14	2	12	85	18	<2	4.6	<0.2	3	0.7	4.4	42.6
THL13-04	X6413	11	2	11	65	12	<2	3.3	<0.2	2	0.6	3.9	36.7
SOF13-01	X6414	8	1	15	67	12	<2	4.2	<0.2	2	0.6	2.3	29.5
SOF13-02	X6415	9	2	<5	67	12	<2	4.4	<0.2	2	0.5	2.2	28.3
SOF13-03	X6416	8	2	14	49	9	<2	3.9	<0.2	1	< 0.5	2.8	24.3
SOF13-04	X6417	8	1	10	53	10	<2	3.1	<0.2	1	< 0.5	2.4	26.9
HF13-01	X6418	10	2	67	72	12	<2	3.3	<0.2	2	0.9	3.4	29.3
CCF13-02	X6419	10	2	11	67	13	<2	3.6	<0.2	2	0.5	3.2	29.8
CCF13-03	X6420	9	1	9	62	13	<2	4.1	<0.2	2	0.5	2.8	29.3
CCF13-04	X6421	10	1	10	67	12	<2	3.1	<0.2	2	0.6	3	27.6
CCF13-05	X6422	13	2	15	89	13	<2	3.3	<0.2	2	0.6	4.3	36.9
CCF13-06	X6423	2	1	<5	15	3	5	0.5	<0.2	<1	<0.5	0.6	6.7
CCF13-09	X6424	10	2	9	66	11	<2	3.1	<0.2	1	< 0.5	2.9	25.1
CCF13-10	X6425	9	2	18	53	11	<2	3.7	<0.2	1	0.7	2.8	29
CCF13-11	X6426	10	2	9	68	10	<2	2.7	<0.2	1	<0.5	2.8	25.5
CCF13-13	X6427	6	1	<5	45	8	<2	2.6	<0.2	1	<0.5	2.3	19
CCF13-15	X6428	8	2	14	55	9	<2	3.4	<0.2	1	<0.5	2.6	22.2
CCF13-16	X6429	13	2	14	86	14	<2	3.6	<0.2	3	<0.5	4.1	34.5
CCF13-17	X6430	10	2	7	84	15	<2	4.4	<0.2	2	<0.5	2.8	30.6

© HISTORIC ENGLAND

APPENDIX 2 (CONTINUED) ELEMENTAL ANALYSIS BY FUSION ICP-MS

Analyte Symbol		Ce	Pr	Nd	Sm	Eu	Gd	Tb	Dy	Ho	Er	Tm
Unit Symbol		ppm	ppm	ppm	ppm	ppm	ppm	ppm	ppm	ppm	ppm	ppm
Detection Limit		0.1	0.05	0.1	0.1	0.05	0.1	0.1	0.1	0.1	0.1	0.05
Field code	Lab code											
OMF13-02	X6410	81.7	9.67	36.7	7	1.41	6.2	1	6.1	1.2	3.6	0.56
HAF13-01	X6411	90.6	10.2	39	7.7	1.45	6.6	1.1	6.6	1.4	3.9	0.59
HAF13-02	X6412	107	10.6	39.5	8.1	1.57	6.9	1.1	6.8	1.4	4	0.62
THL13-04	X6413	77.6	10.2	41.3	9.1	1.83	7.9	1.2	7.4	1.5	4.1	0.61
SOF13-01	X6414	57.4	6.72	24.8	4.8	0.89	4.2	0.7	4.3	0.9	2.7	0.43
SOF13-02	X6415	56.7	6.55	24.6	4.6	0.85	4.1	0.7	4.3	0.9	2.7	0.45
SOF13-03	X6416	65.3	6.43	25.1	5.2	1.1	4.5	0.7	4.2	0.8	2.3	0.35
SOF13-04	X6417	45.8	6.39	24.4	4.9	0.99	4.3	0.7	4.1	0.8	2.2	0.34
HF13-01	X6418	56	7.06	26.6	5.2	1.02	4.4	0.8	4.5	0.9	2.7	0.42
CCF13-02	X6419	60.3	7.14	26.6	5.3	1.06	4.5	0.7	4.4	0.9	2.6	0.41
CCF13-03	X6420	59.4	7.1	26.6	5.3	0.99	4.6	0.7	4.5	0.9	2.7	0.42
CCF13-04	X6421	55.7	6.61	24.9	4.9	0.96	4.3	0.7	4.5	0.9	2.6	0.39
CCF13-05	X6422	72.5	9.11	35.3	6.9	1.37	6	1	5.9	1.2	3.5	0.52
CCF13-06	X6423	11.4	1.62	5.9	1.1	0.24	1	0.2	0.9	0.2	0.5	0.07
CCF13-09	X6424	51.8	6.12	23.5	4.7	0.91	4.1	0.7	4.2	0.8	2.4	0.37
CCF13-10	X6425	59.3	7.55	29.8	5.8	1.21	4.9	0.8	4.6	0.9	2.7	0.42
CCF13-11	X6426	51.7	6.12	22.8	4.5	0.92	4.1	0.7	4	0.8	2.4	0.38
CCF13-13	X6427	37.8	4.56	17.5	3.2	0.67	2.8	0.4	2.7	0.5	1.6	0.26
CCF13-15	X6428	46.1	5.45	20.8	4.2	0.86	3.5	0.6	3.4	0.7	2.1	0.34
CCF13-16	X6429	72.7	8.31	31.2	6.3	1.24	5.4	0.9	5.6	1.1	3.2	0.49
CCF13-17	X6430	62.4	7.09	26.7	5	0.91	4.2	0.7	4.5	0.9	2.7	0.44

© HISTORIC ENGLAND

APPENDIX 2 (CONTINUED) ELEMENTAL ANALYSIS BY FUSION ICP-MS

Analyte Symbol		Lu	Hf	Ta	W	Tl	Pb	Bi	Th	U	Yb
Unit Symbol		ppm	ppm	ppm	ppm	ppm	ppm	ppm	ppm	ppm	ppm
Detection Limit		0.04	0.2	0.1	1	0.1	5	0.4	0.1	0.1	0.1
Field code	Lab code										
OMF13-02	X6410	0.57	11.1	1.1	4	0.3	20	< 0.4	10.7	3	3.7
HAF13-01	X6411	0.64	12.8	1.2	3	0.3	23	< 0.4	13.2	2.9	4.1
HAF13-02	X6412	0.69	14.5	1.4	4	0.2	22	< 0.4	11.7	2.8	4.2
THL13-04	X6413	0.64	10.6	0.8	3	0.2	19	< 0.4	9.3	2.1	4.2
SOF13-01	X6414	0.47	12.4	0.9	3	0.2	24	< 0.4	8.5	2.4	2.9
SOF13-02	X6415	0.48	12.7	1	3	0.1	17	< 0.4	8.8	2.5	3
SOF13-03	X6416	0.39	11.2	0.6	2	< 0.1	16	< 0.4	6.5	1.5	2.5
SOF13-04	X6417	0.38	9	0.7	2	< 0.1	12	< 0.4	6.3	1.9	2.4
HF13-01	X6418	0.43	9.5	0.9	3	0.2	24	< 0.4	8.8	2.4	2.7
CCF13-02	X6419	0.43	10.1	1.1	3	0.1	18	< 0.4	8.9	2.5	2.8
CCF13-03	X6420	0.47	11.8	0.9	2	0.1	14	< 0.4	8.9	2.6	2.9
CCF13-04	X6421	0.45	9.4	1	2	0.1	14	< 0.4	8.2	2.4	2.7
CCF13-05	X6422	0.54	10.5	1	3	0.2	22	< 0.4	10.8	2.7	3.3
CCF13-06	X6423	0.07	1.4	0.2	1	< 0.1	5	< 0.4	1.4	0.4	0.5
CCF13-09	X6424	0.4	9.2	0.9	2	< 0.1	14	< 0.4	7.8	2.3	2.6
CCF13-10	X6425	0.44	10.8	0.7	2	< 0.1	16	< 0.4	7.4	2	2.8
CCF13-11	X6426	0.38	8.7	0.8	2	0.1	14	< 0.4	7.9	2.4	2.4
CCF13-13	X6427	0.27	8.3	0.6	2	< 0.1	9	< 0.4	5	1.4	1.7
CCF13-15	X6428	0.36	10.5	1.2	2	< 0.1	13	< 0.4	6.2	1.9	2.3
CCF13-16	X6429	0.52	11.3	1	52	0.2	21	< 0.4	10.9	2.9	3.4
CCF13-17	X6430	0.49	13.5	1.1	3	0.2	17	< 0.4	10.4	2.9	3

APPENDIX 3: TYPICAL OSL SHINE DOWN CURVES, GROWTH CURVES, AND D_E DISTRIBUTIONS

X6410

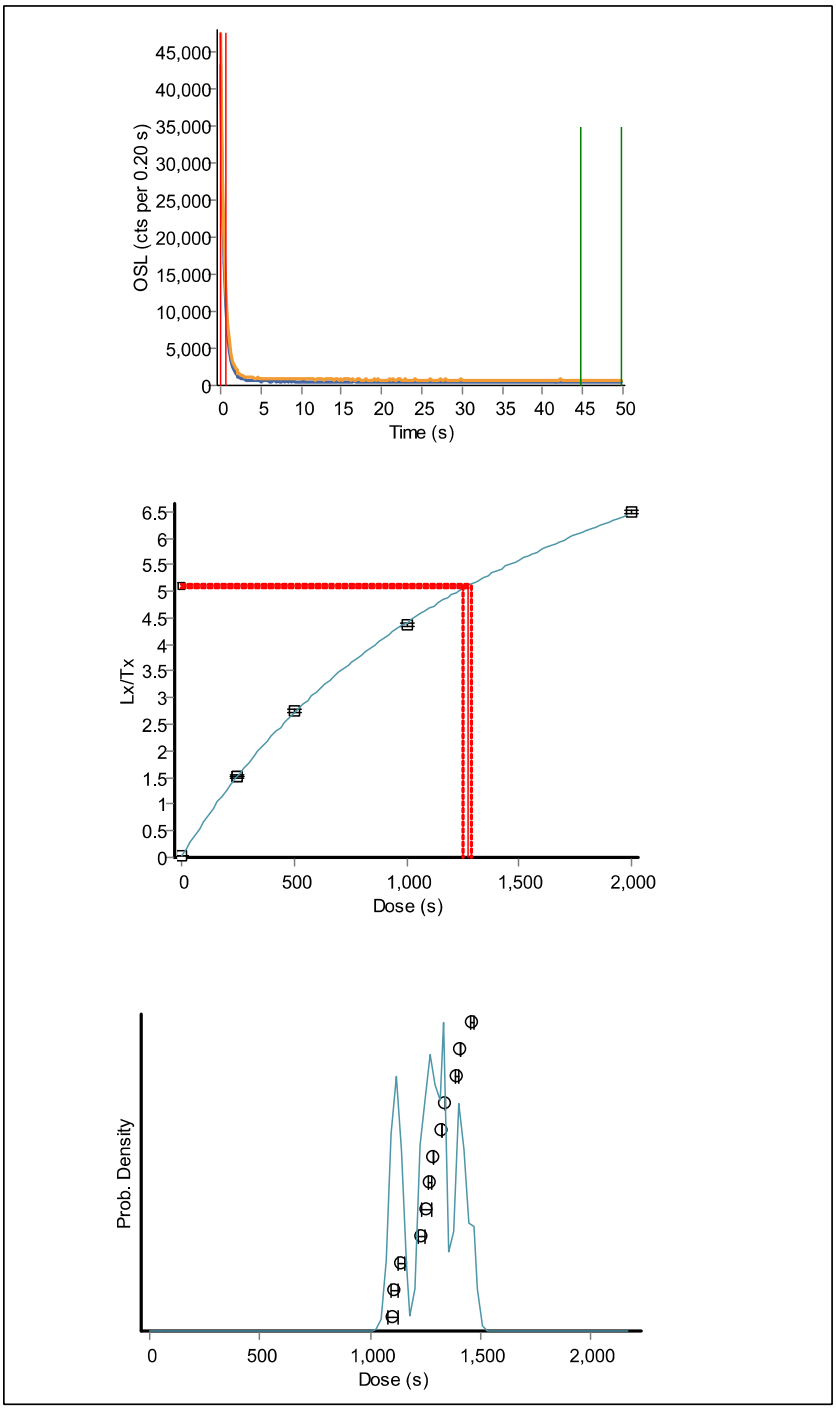

APPENDIX 3 (CONTINUED): TYPICAL OSL SHINE DOWN CURVES, GROWTH CURVES, AND D_E DISTRIBUTIONS

X6411

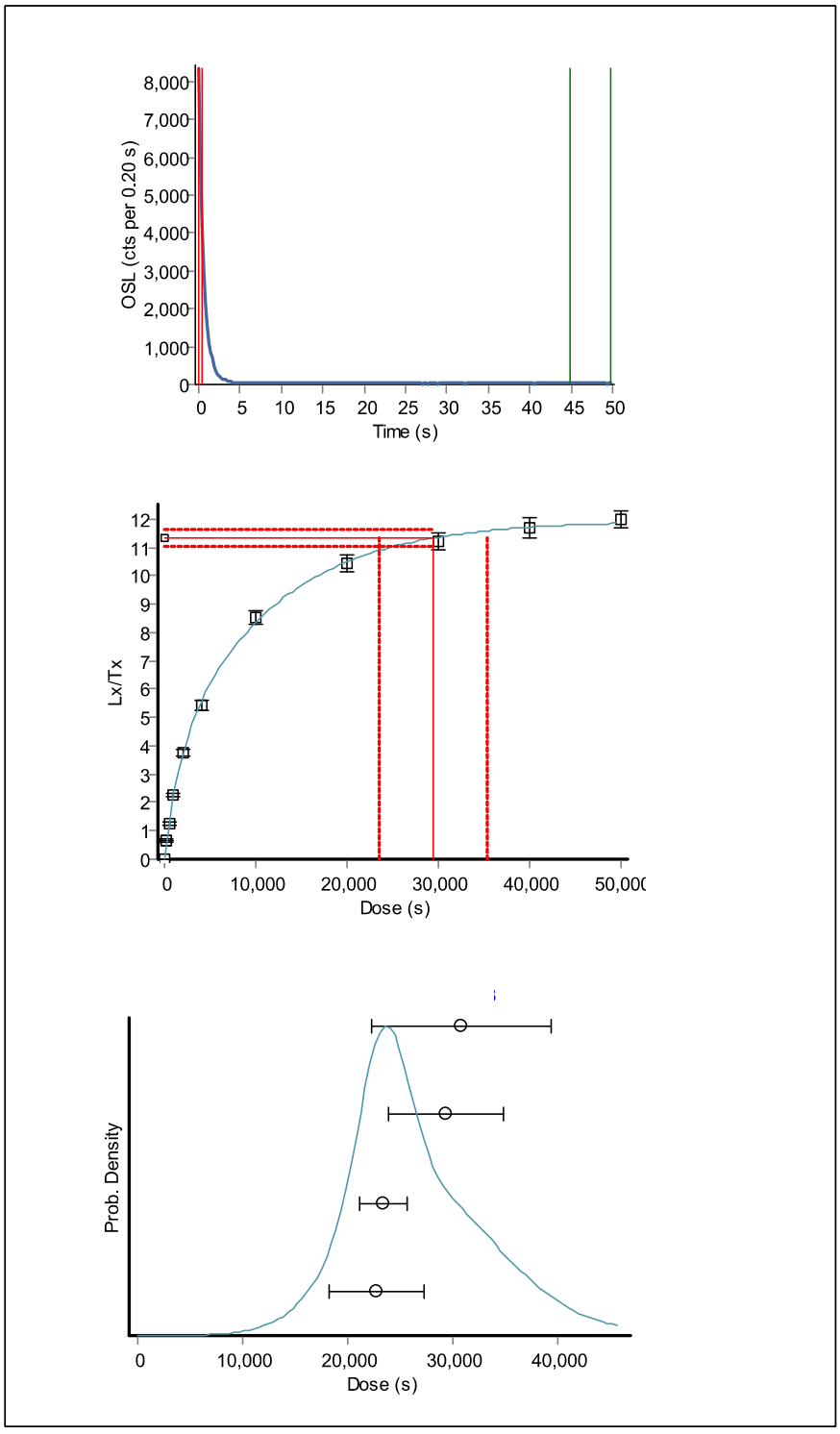

APPENDIX 3 (CONTINUED): TYPICAL OSL SHINE DOWN CURVES, GROWTH CURVES, AND D_E DISTRIBUTIONS

X6412

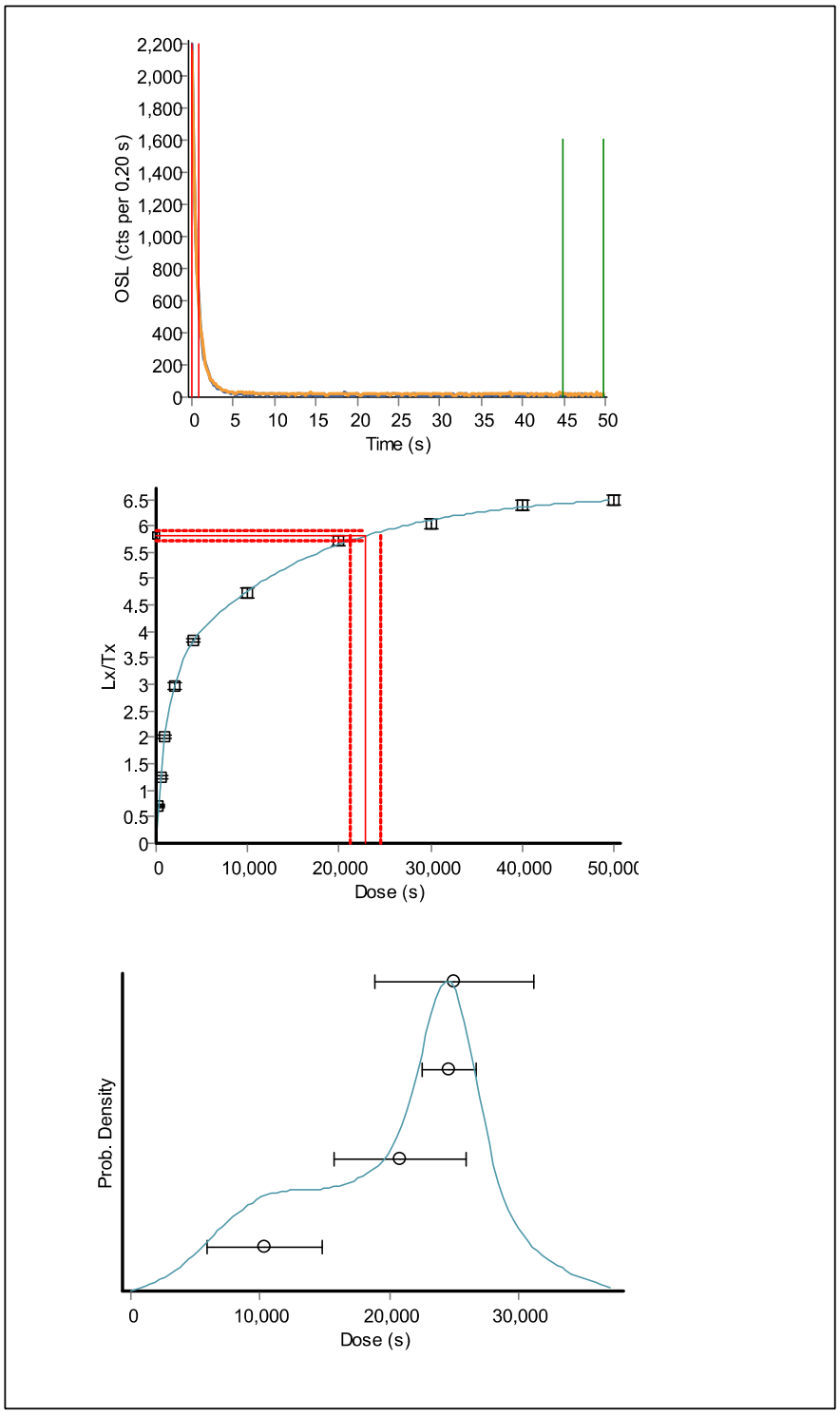

APPENDIX 3 (CONTINUED): TYPICAL OSL SHINE DOWN CURVES, GROWTH CURVES, AND D_E DISTRIBUTIONS

X6413

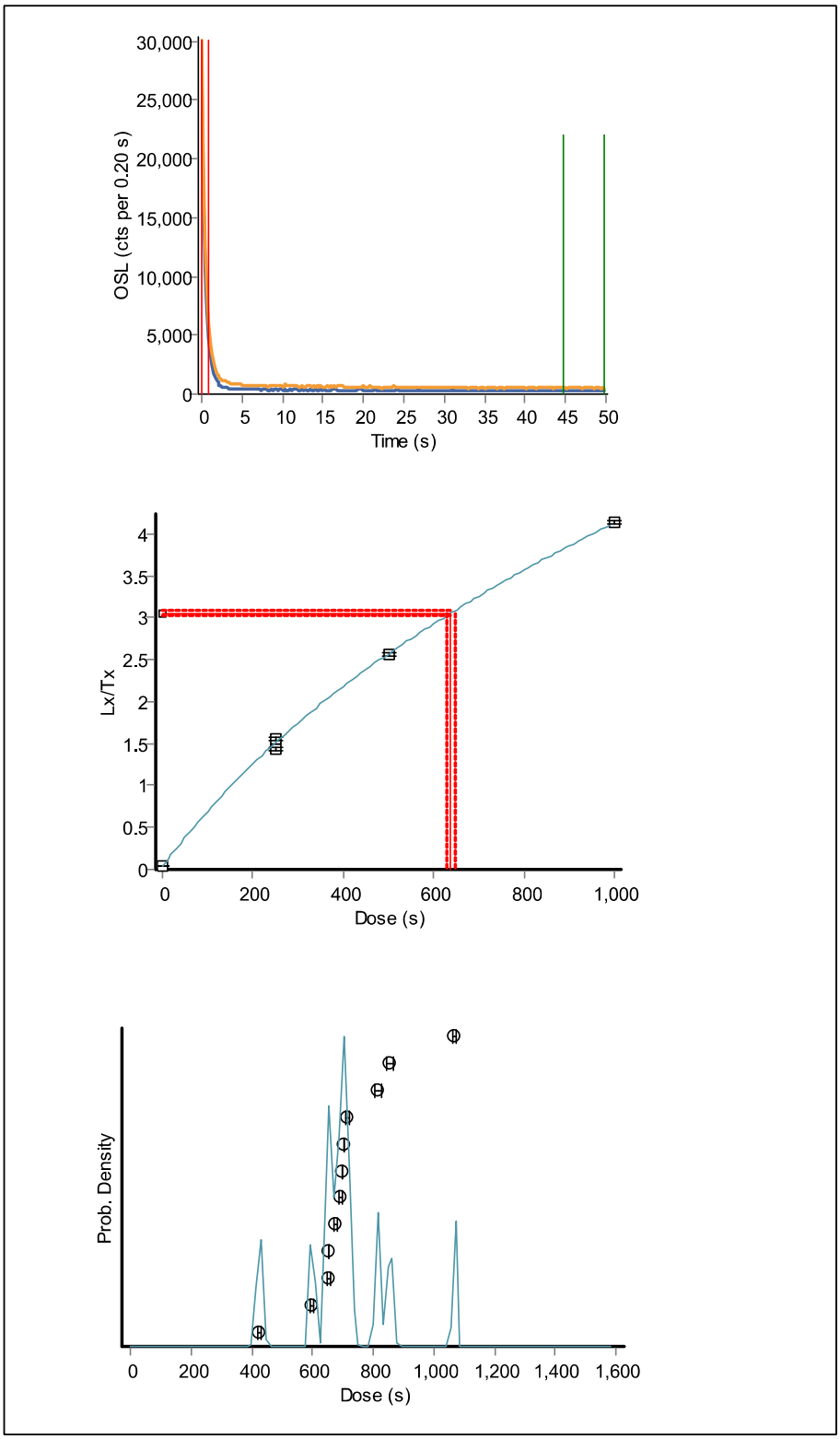

APPENDIX 3 (CONTINUED): TYPICAL OSL SHINE DOWN CURVES, GROWTH CURVES, AND D_E DISTRIBUTIONS

X6414

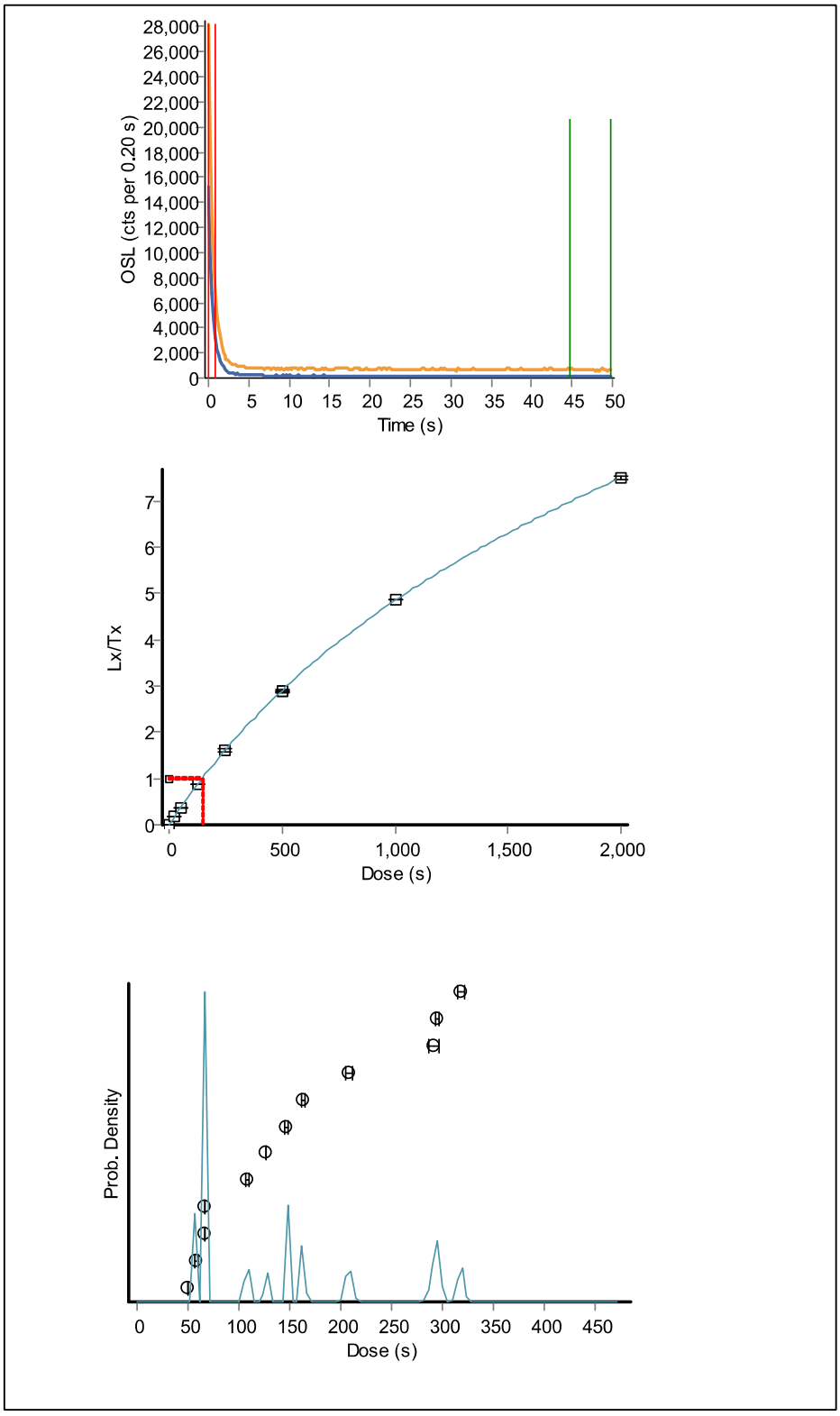

APPENDIX 3 (CONTINUED): TYPICAL OSL SHINE DOWN CURVES, GROWTH CURVES, AND D_E DISTRIBUTIONS

X6415

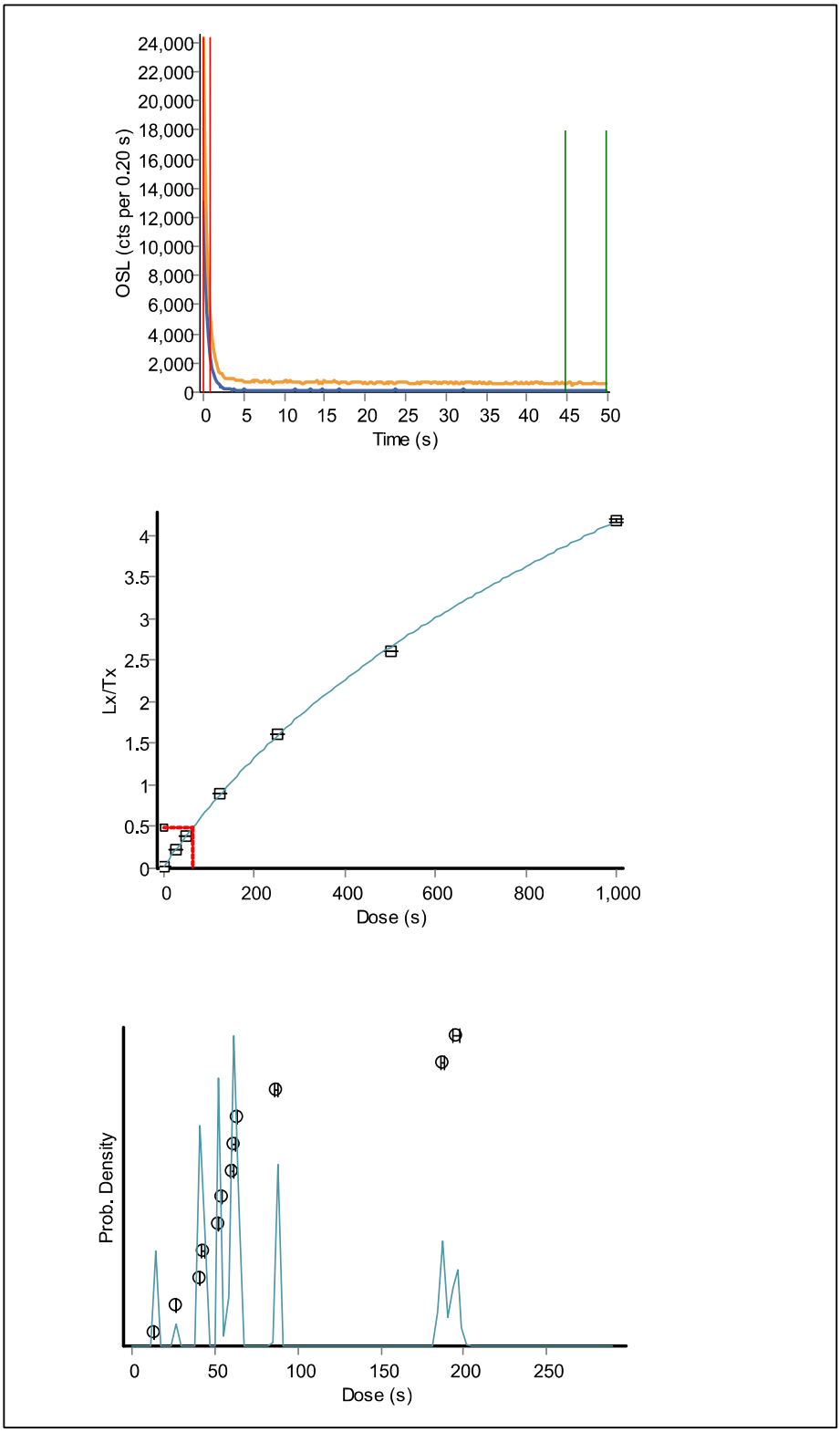

APPENDIX 3 (CONTINUED): TYPICAL OSL SHINE DOWN CURVES, GROWTH CURVES, AND D_E DISTRIBUTIONS

X6416

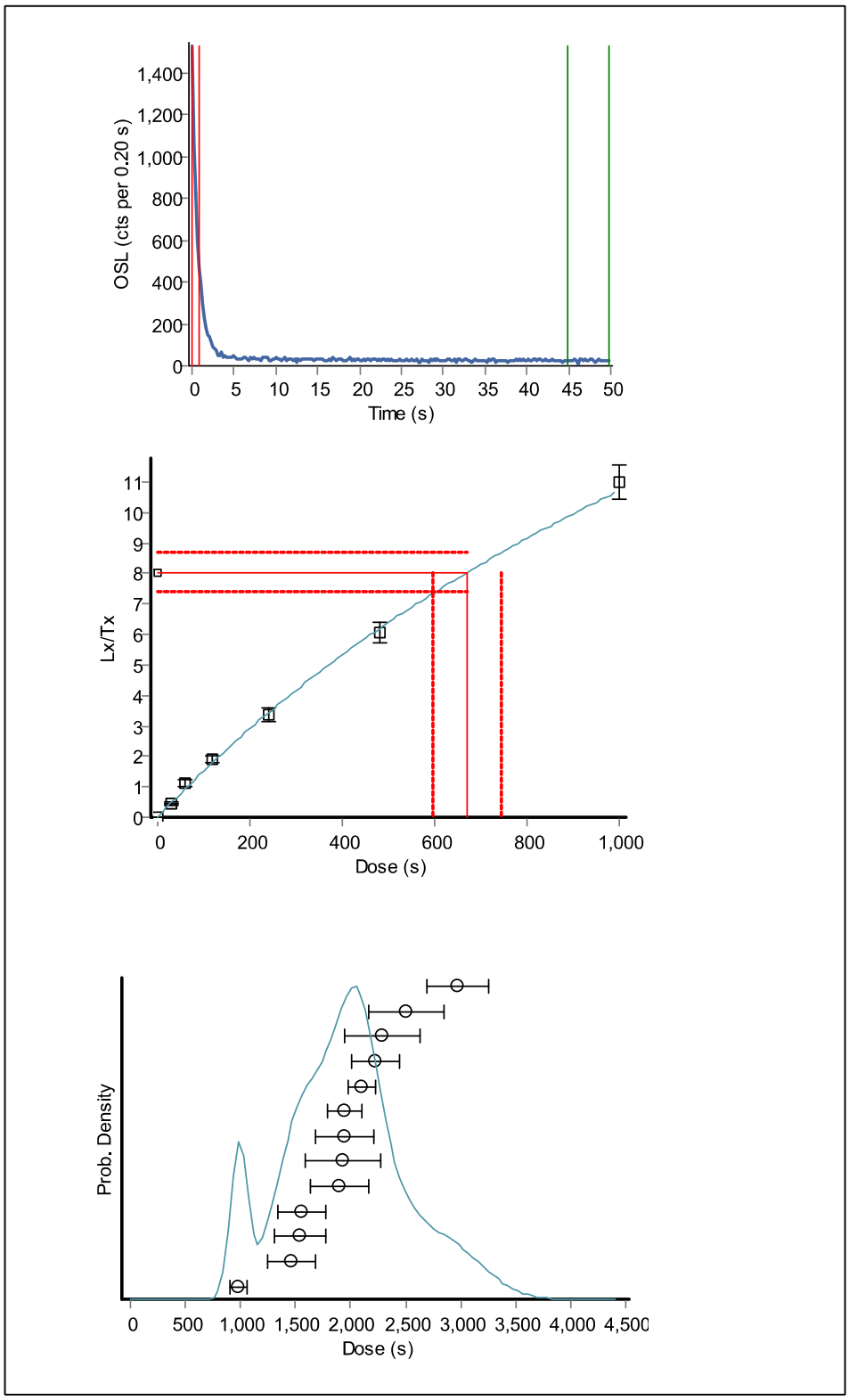

APPENDIX 3 (CONTINUED): TYPICAL OSL SHINE DOWN CURVES, GROWTH CURVES, AND D_E DISTRIBUTIONS

X6417

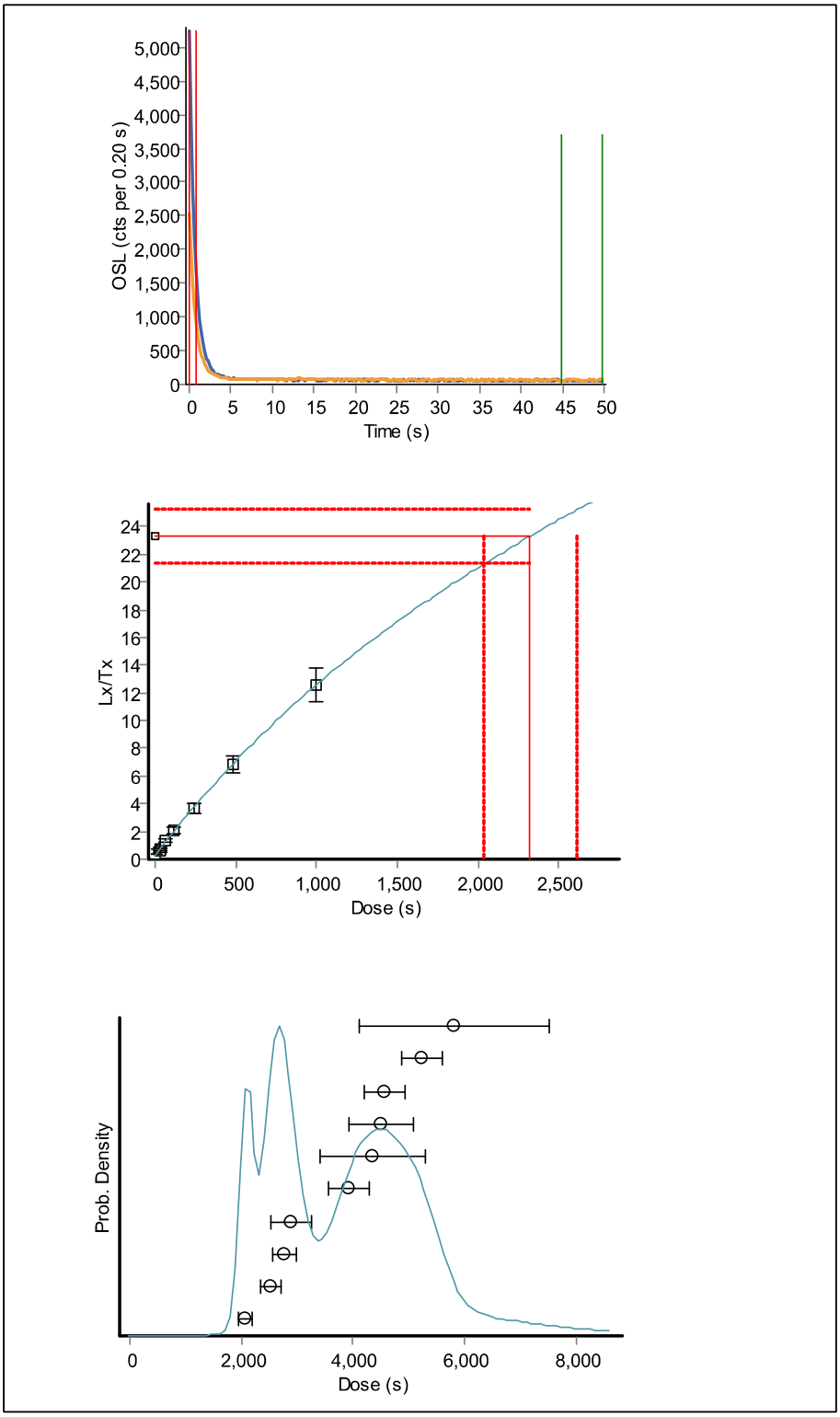

APPENDIX 3 (CONTINUED): TYPICAL OSL SHINE DOWN CURVES, GROWTH CURVES, AND D_E DISTRIBUTIONS

X6418

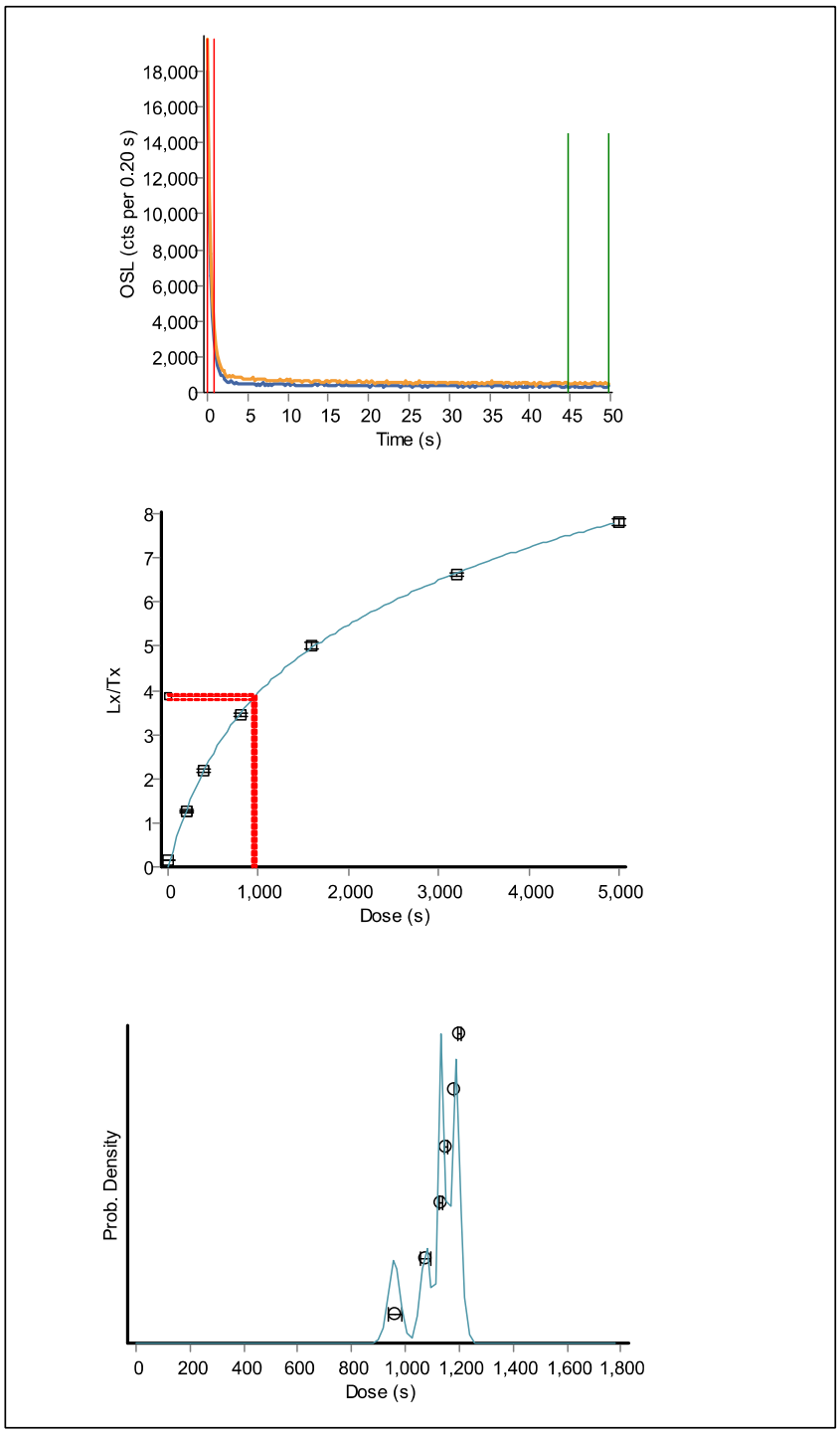

APPENDIX 3 (CONTINUED): TYPICAL OSL SHINE DOWN CURVES, GROWTH CURVES, AND D_E DISTRIBUTIONS

X6419

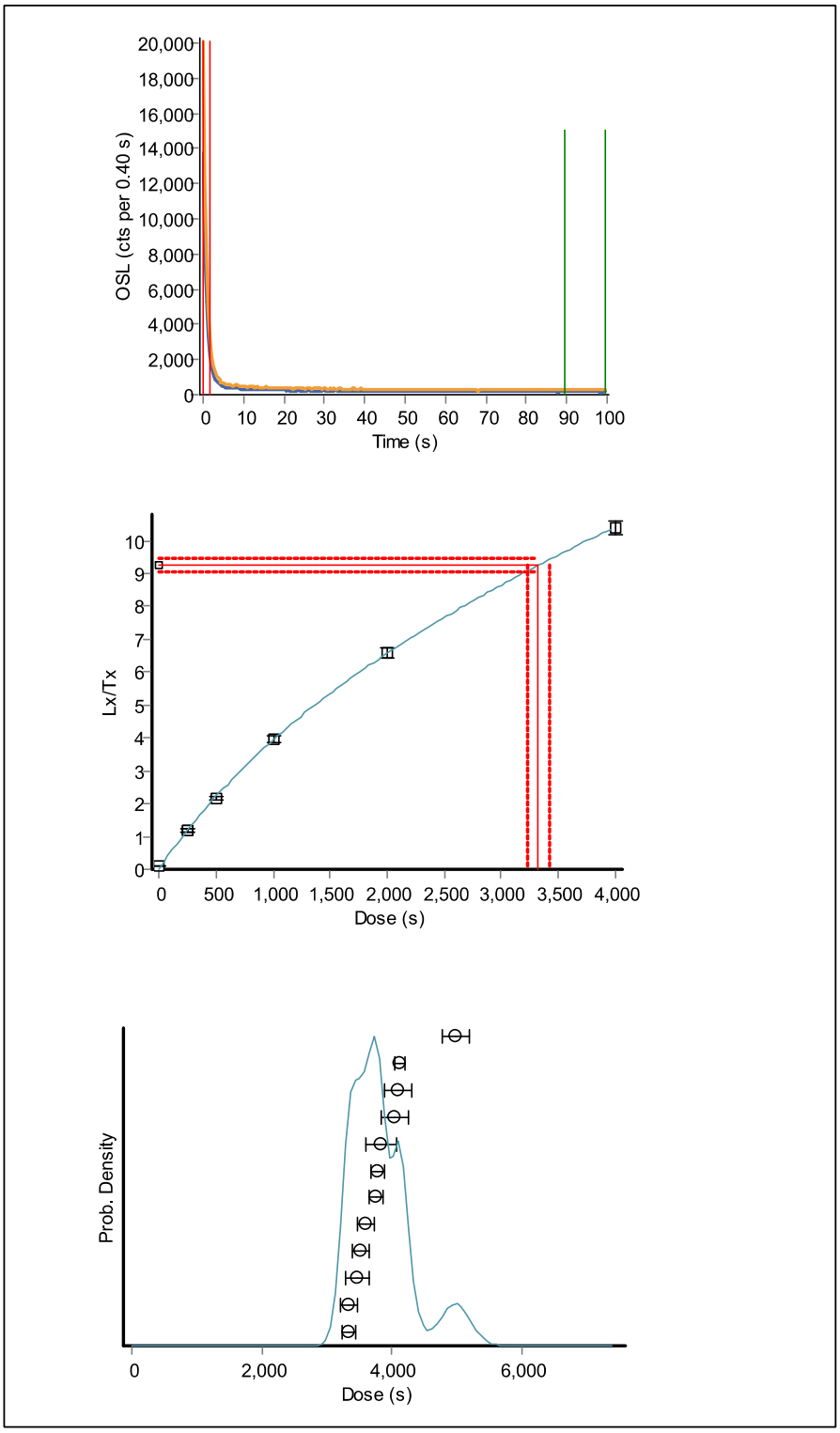

APPENDIX 3 (CONTINUED): TYPICAL OSL SHINE DOWN CURVES, GROWTH CURVES, AND DE DISTRIBUTIONS

X6420

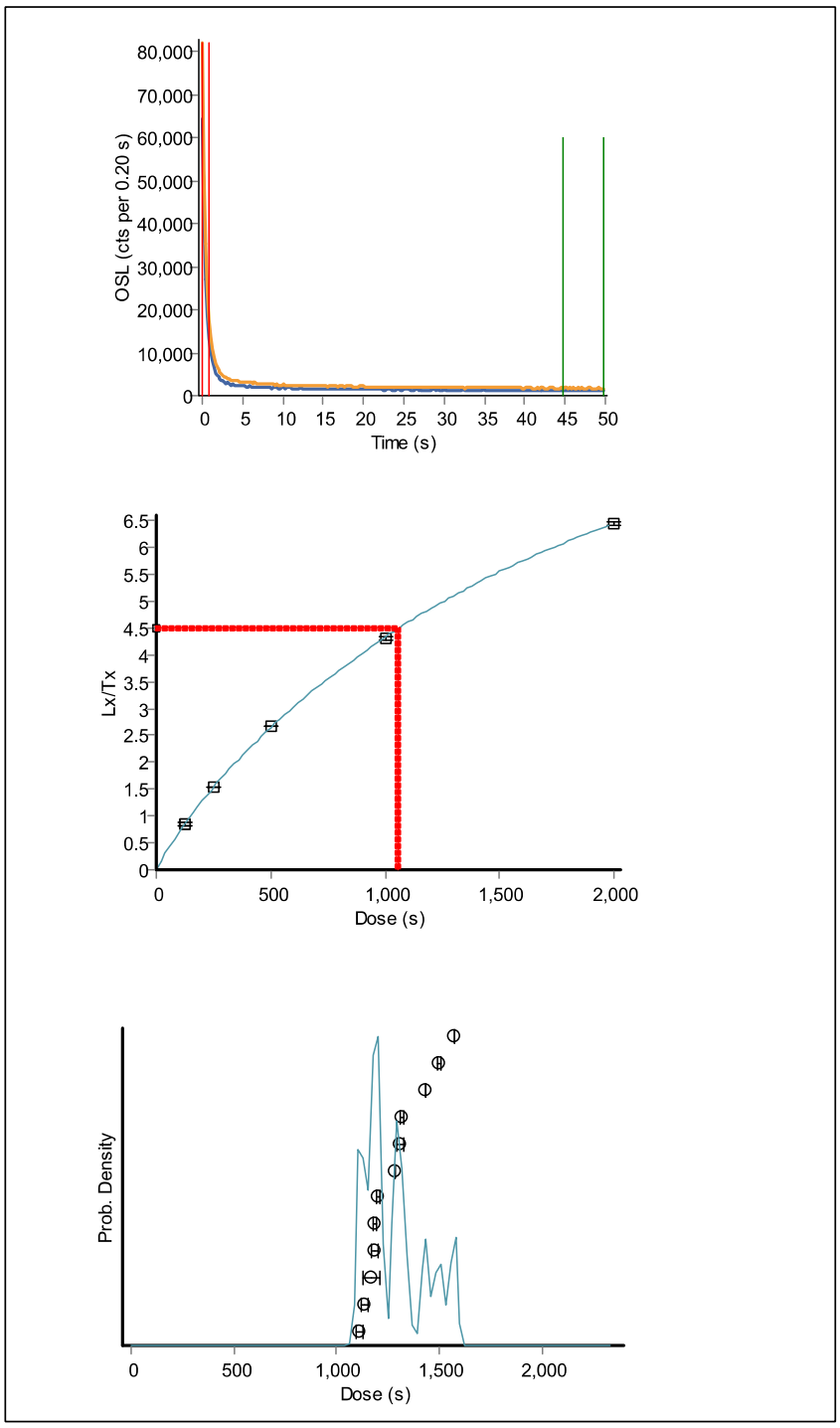

APPENDIX 3 (CONTINUED): TYPICAL OSL SHINE DOWN CURVES, GROWTH CURVES, AND DE DISTRIBUTIONS

X6421

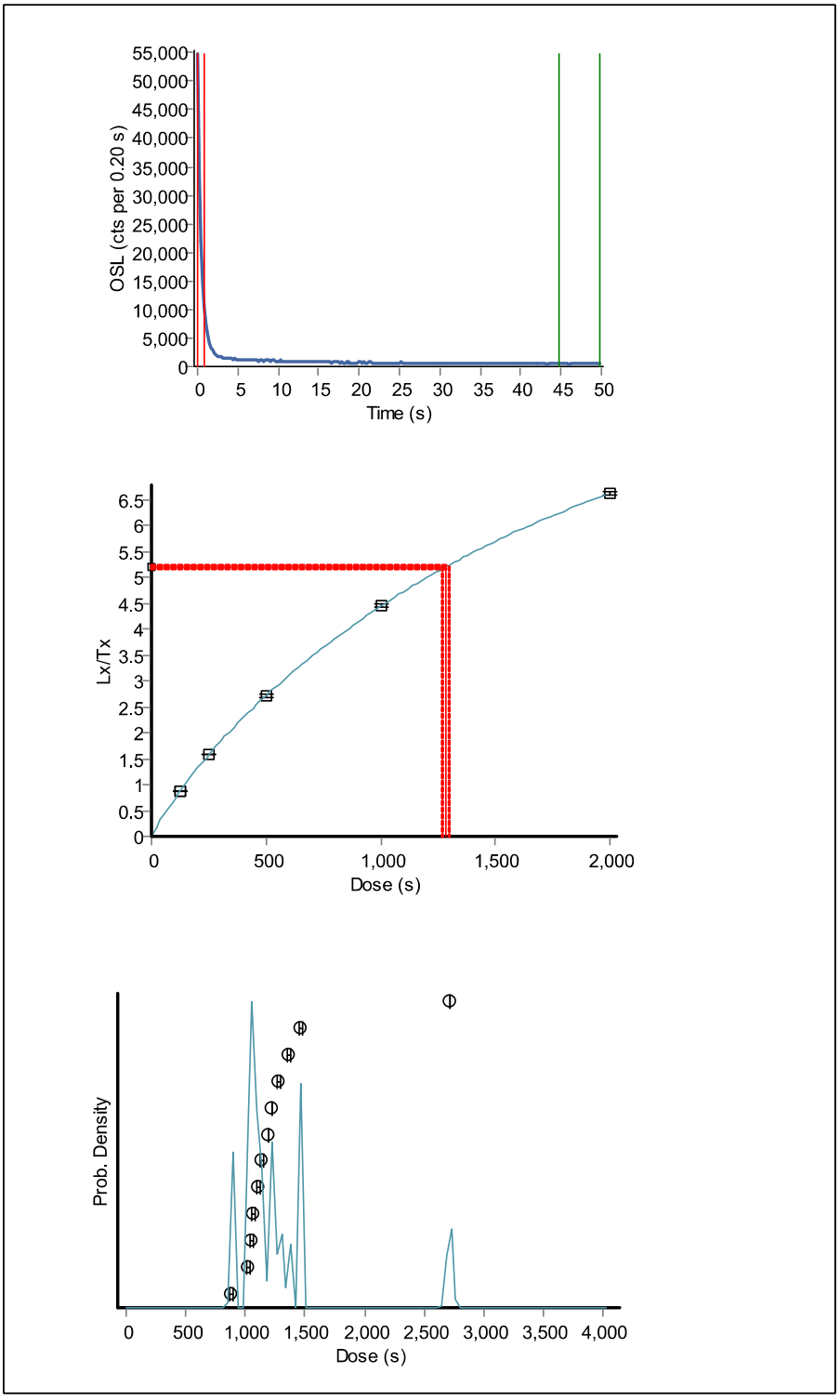

APPENDIX 3 (CONTINUED): TYPICAL OSL SHINE DOWN CURVES, GROWTH CURVES, AND D_E DISTRIBUTIONS

X6422

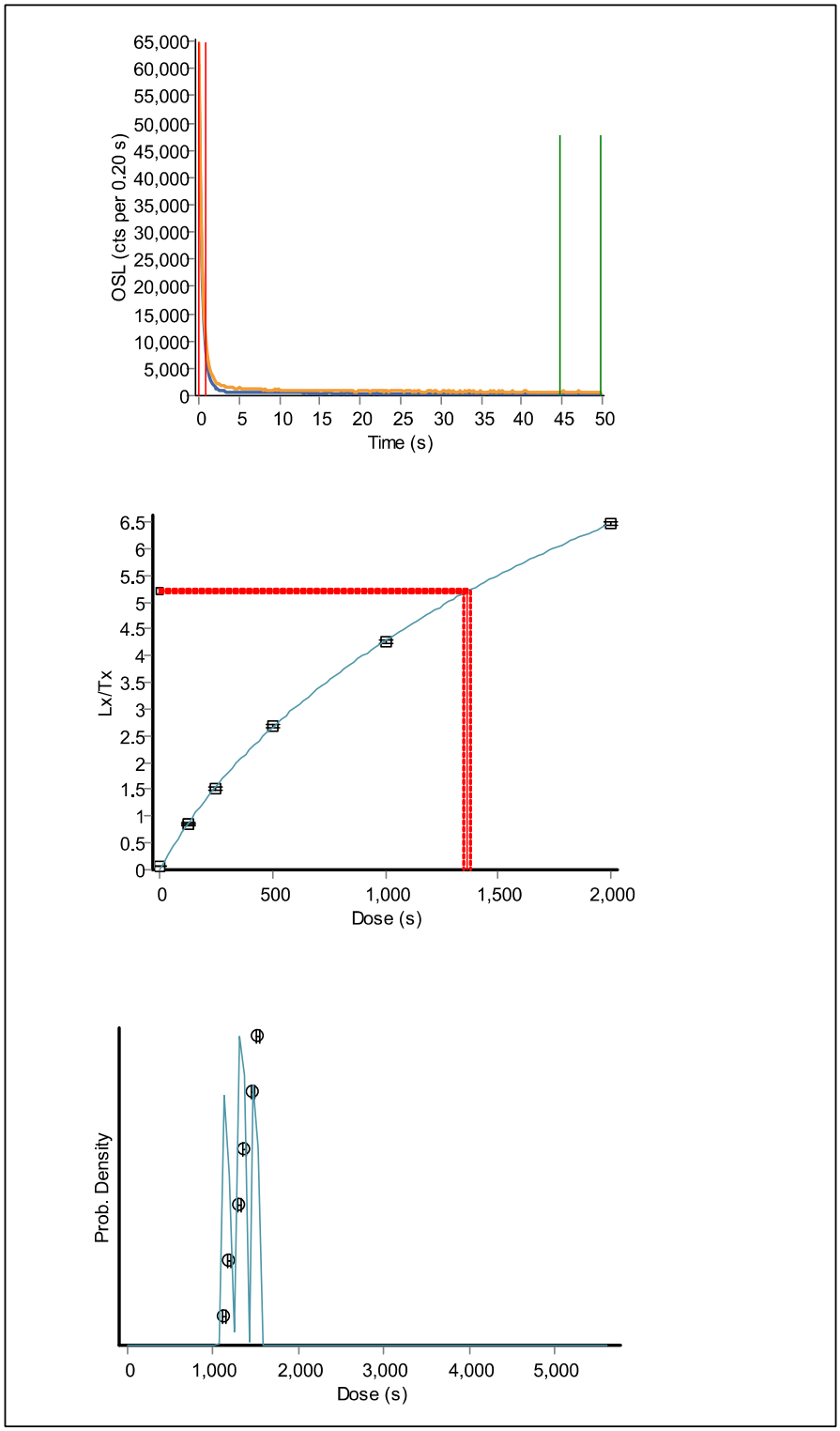

APPENDIX 3 (CONTINUED): TYPICAL OSL SHINE DOWN CURVES, GROWTH CURVES, AND D_E DISTRIBUTIONS

X6423

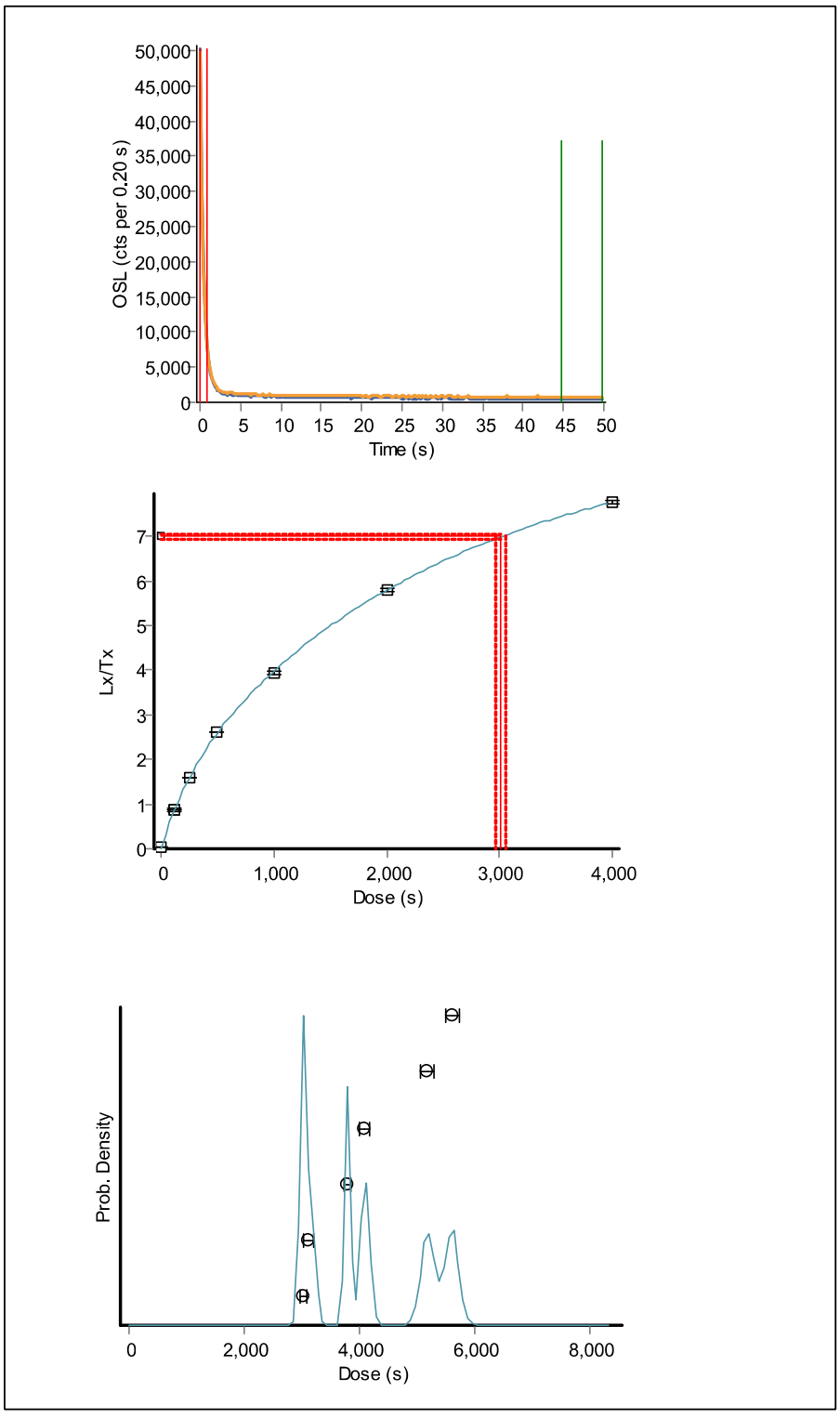

APPENDIX 3 (CONTINUED): TYPICAL OSL SHINE DOWN CURVES, GROWTH CURVES, AND D_E DISTRIBUTIONS

X6424

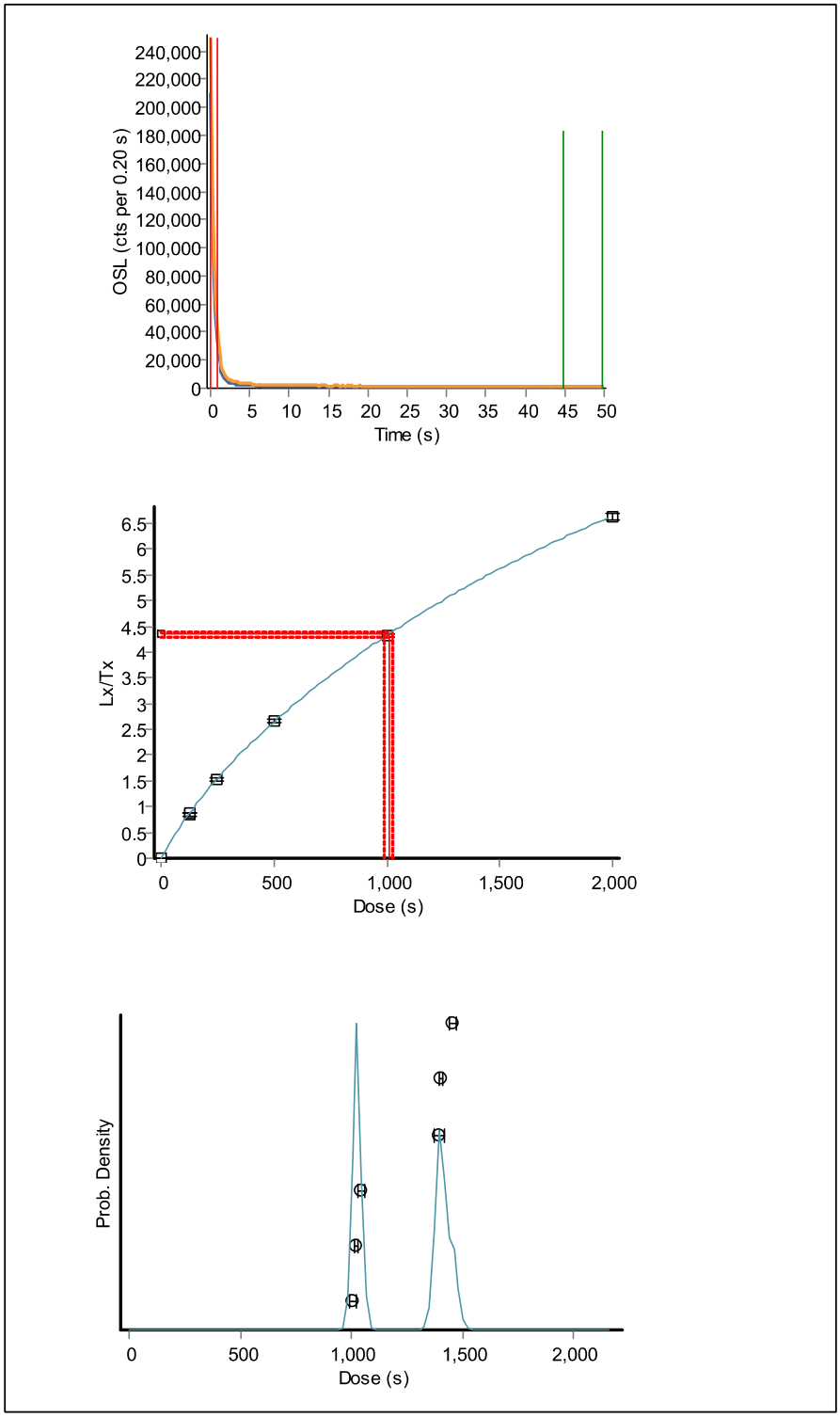

APPENDIX 3 (CONTINUED): TYPICAL OSL SHINE DOWN CURVES, GROWTH CURVES, AND D_E DISTRIBUTIONS

X6425

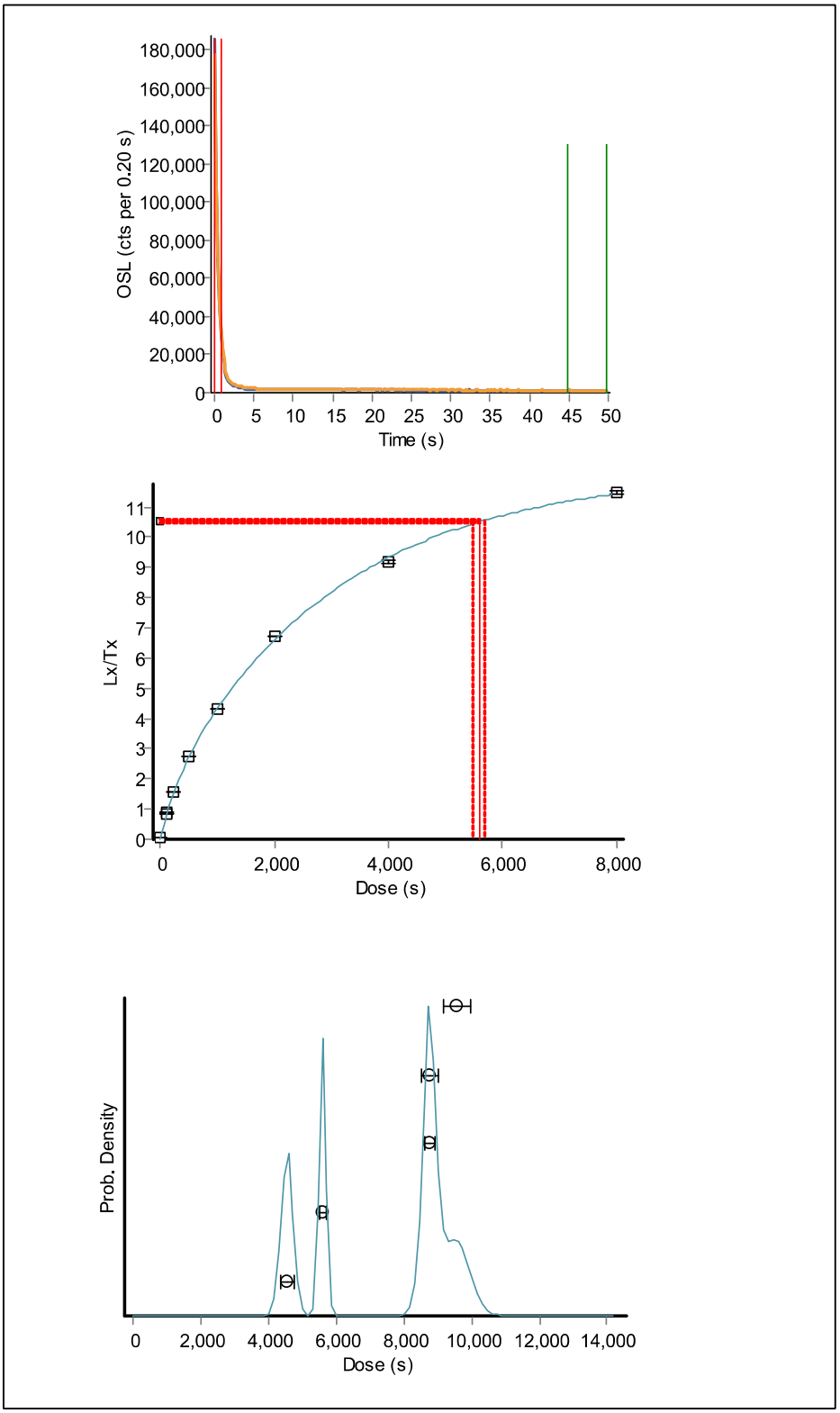

APPENDIX 3 (CONTINUED): TYPICAL OSL SHINE DOWN CURVES, GROWTH CURVES, AND D_E DISTRIBUTIONS

X6426

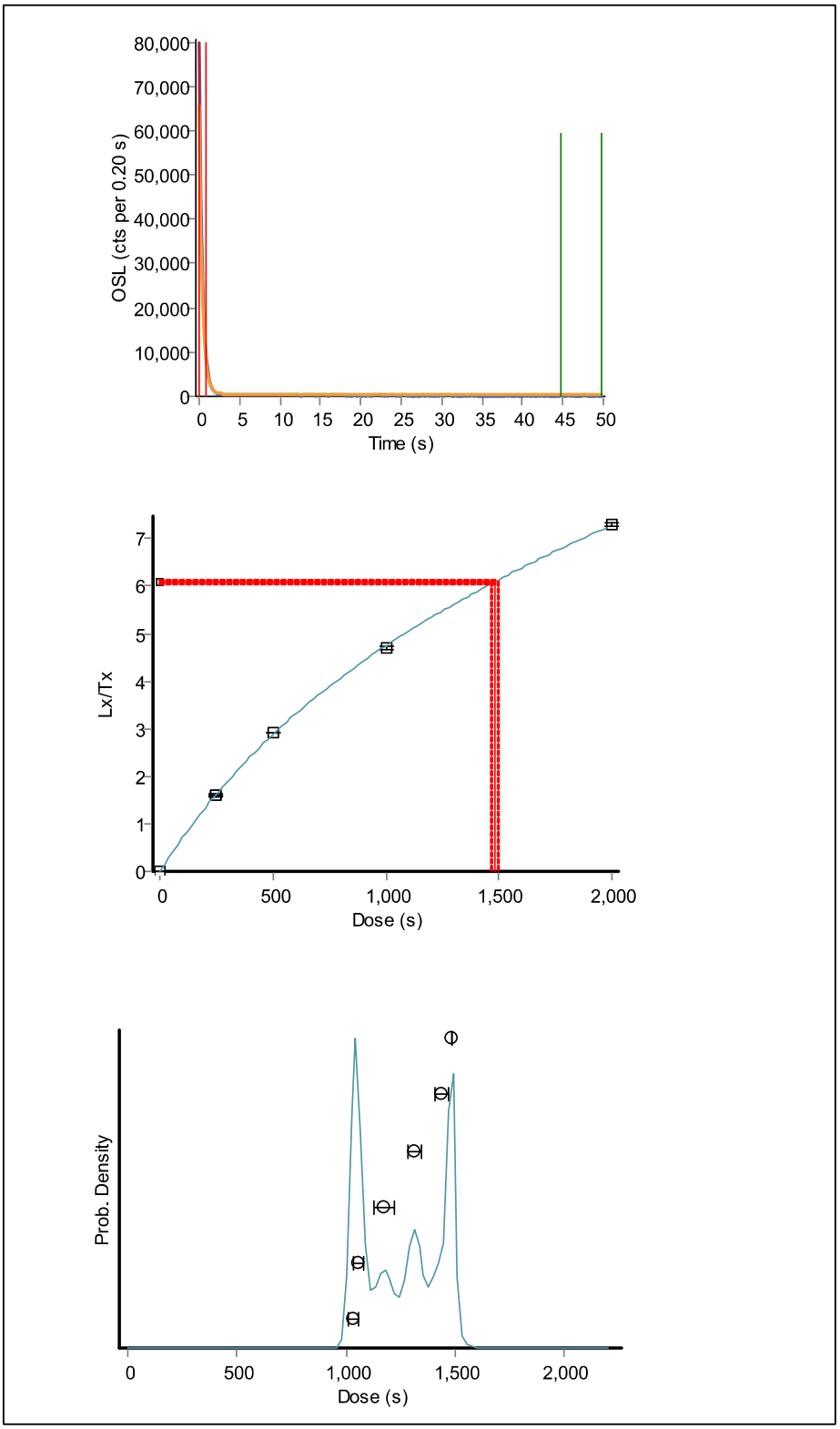

APPENDIX 3 (CONTINUED): TYPICAL OSL SHINE DOWN CURVES, GROWTH CURVES, AND D_E DISTRIBUTIONS

X6427

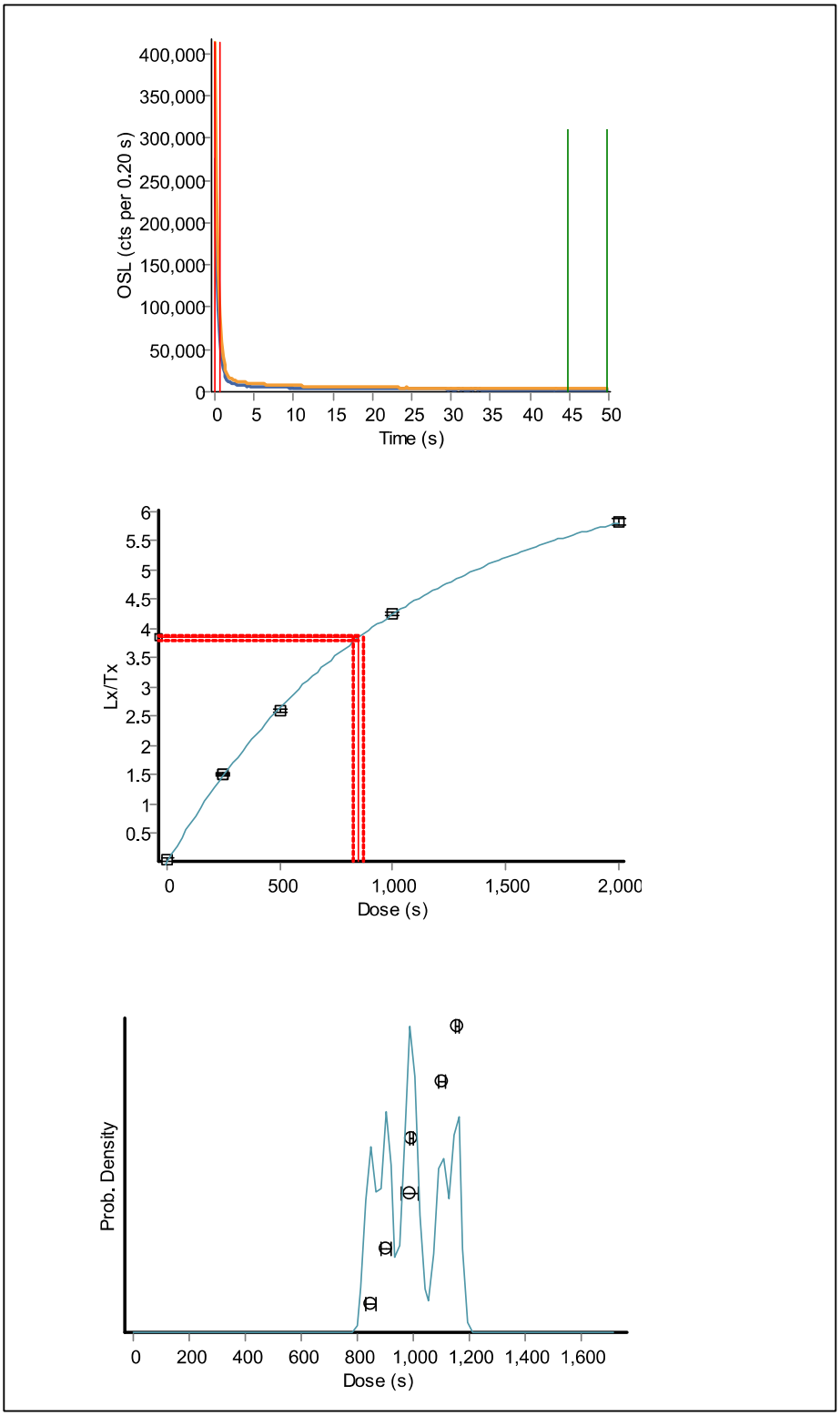

APPENDIX 3 (CONTINUED): TYPICAL OSL SHINE DOWN CURVES, GROWTH CURVES, AND D_E DISTRIBUTIONS

X6428

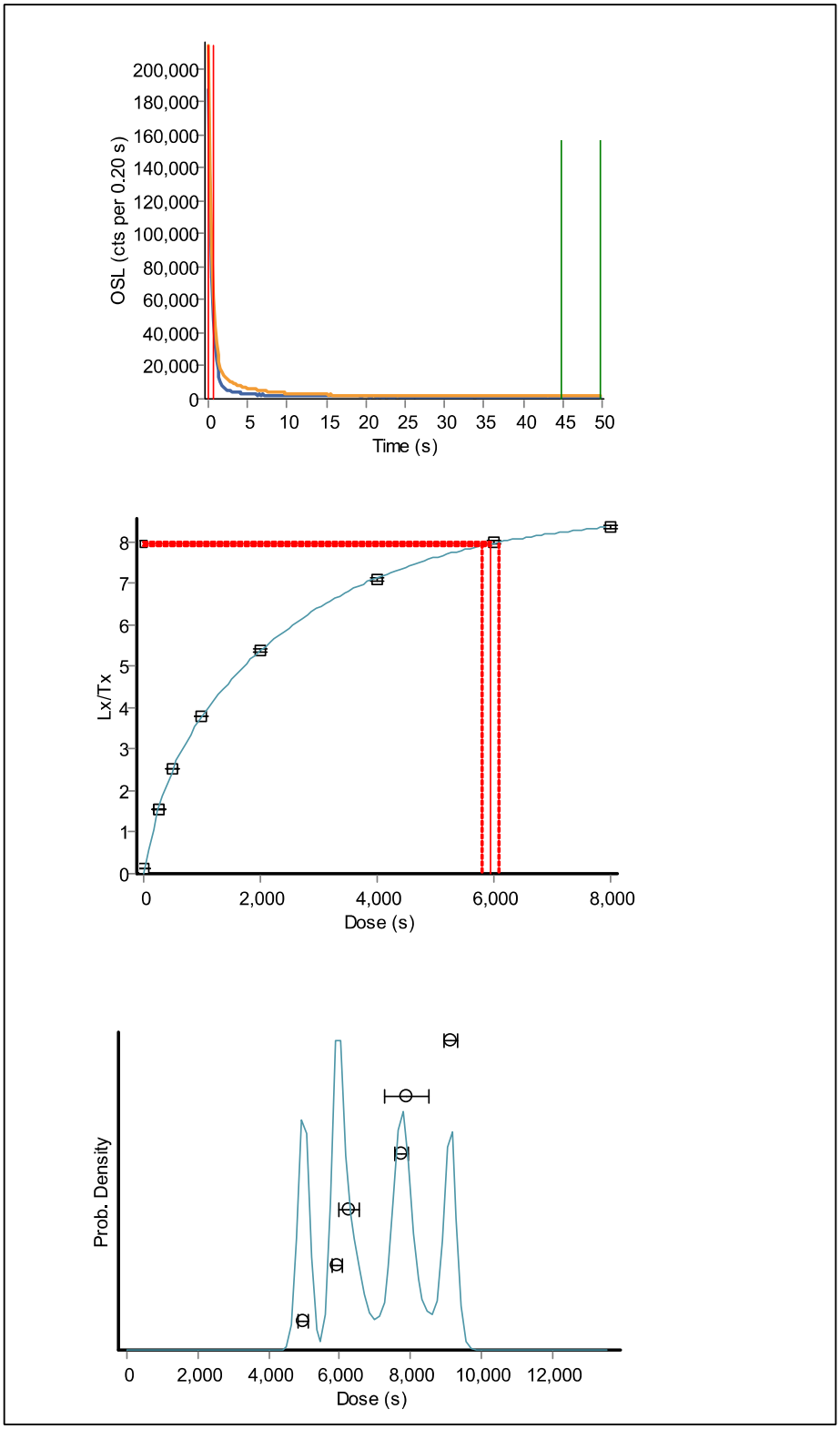

APPENDIX 3 (CONTINUED): TYPICAL OSL SHINE DOWN CURVES, GROWTH CURVES, AND D_E DISTRIBUTIONS

X6429

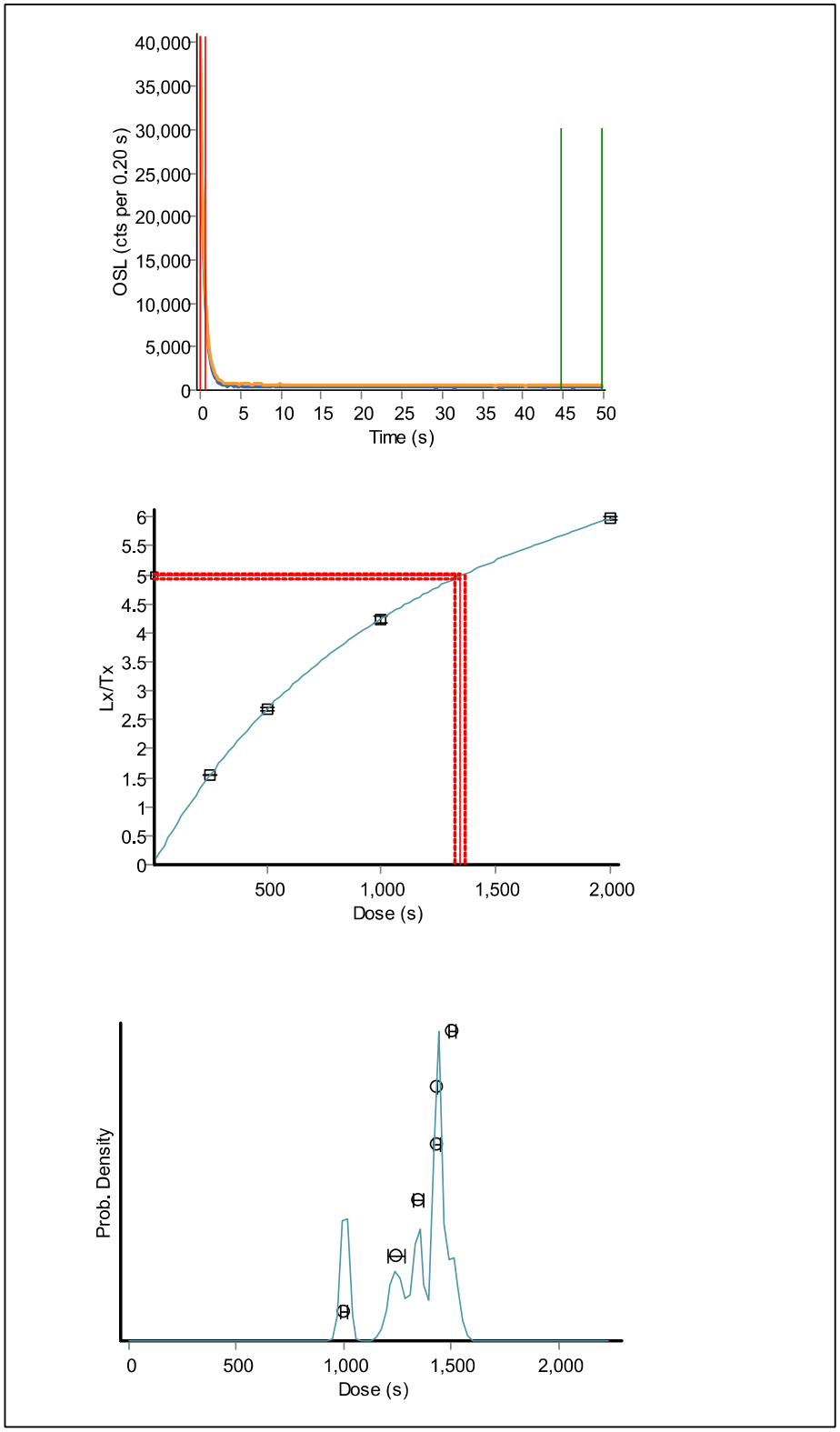

APPENDIX 3 (CONTINUED): TYPICAL OSL SHINE DOWN CURVES, GROWTH CURVES, AND D_E DISTRIBUTIONS

X6430

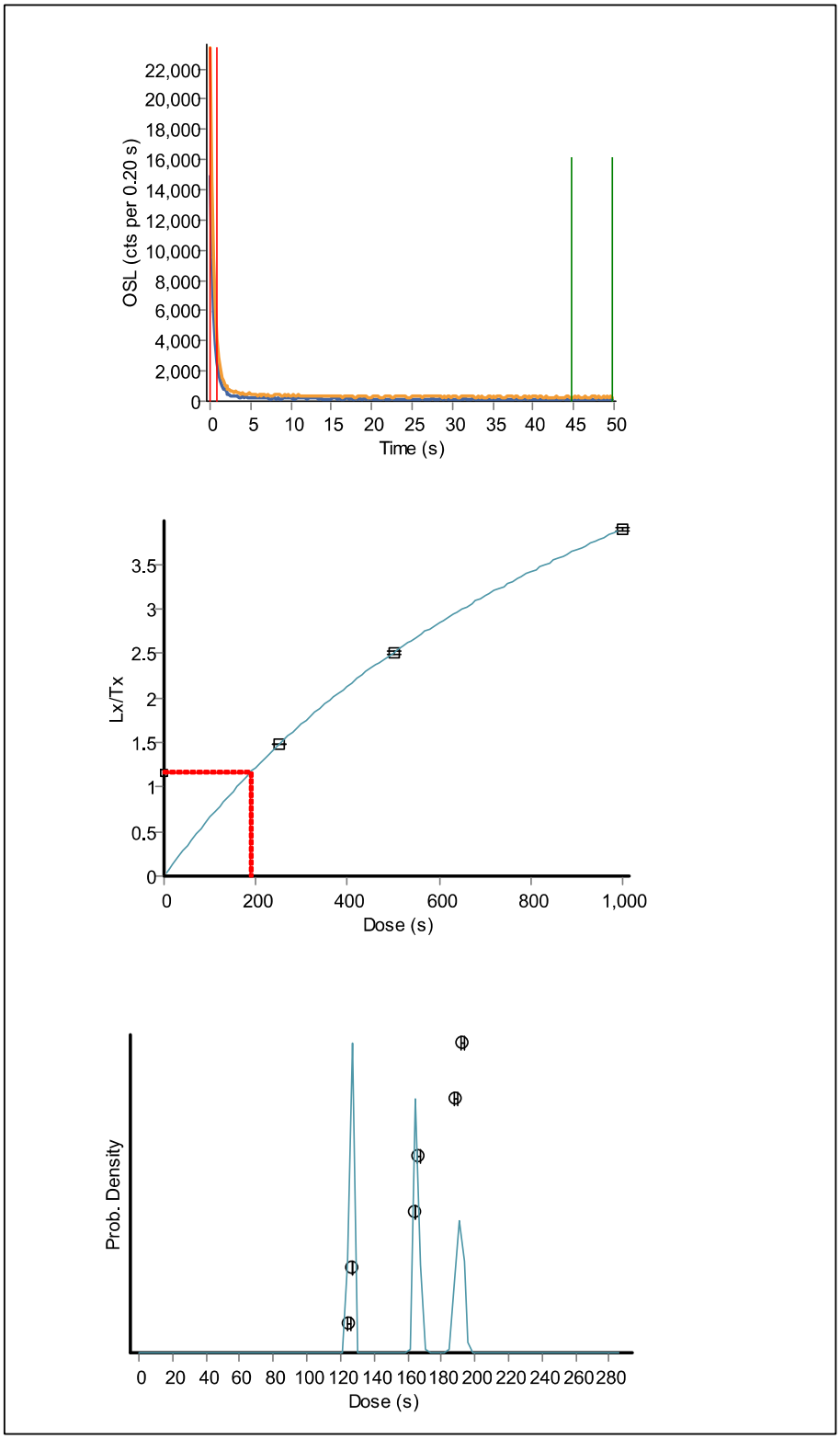

Historic England Research and the Historic Environment

We are the public body that looks after England's historic environment. We champion historic places, helping people understand, value and care for them.

A good understanding of the historic environment is fundamental to ensuring people appreciate and enjoy their heritage and provides the essential first step towards its effective protection.

Historic England works to improve care, understanding and public enjoyment of the historic environment. We undertake and sponsor authoritative research. We develop new approaches to interpreting and protecting heritage and provide high quality expert advice and training.

We make the results of our work available through the Historic England Research Report Series, and through journal publications and monographs. Our online magazine Historic England Research which appears twice a year, aims to keep our partners within and outside Historic England up-to-date with our projects and activities.

A full list of Research Reports, with abstracts and information on how to obtain copies, may be found on www.HistoricEngland.org.uk/researchreports

Some of these reports are interim reports, making the results of specialist investigations available in advance of full publication. They are not usually subject to external refereeing, and their conclusions may sometimes have to be modified in the light of information not available at the time of the investigation.

Where no final project report is available, you should consult the author before citing these reports in any publication. Opinions expressed in these reports are those of the author(s) and are not necessarily those of Historic England.

The Research Report Series incorporates reports by the expert teams within the Investigation& Analysis Division of the Heritage Protection Department of Historic England, alongside contributions from other parts of the organisation. It replaces the former Centre for Archaeology Reports Series, the Archaeological Investigation Report Series, the Architectural Investigation Report Series, and the Research Department Report Series

ISSN 2059-4453 (Online)